TURUN YLIOPISTON JULKAISUJA
ANNALES UNIVERSITATIS TURKUENSIS

SARJA - SER. A I OSA - TOM. 388

ASTRONOMICA - CHEMICA - PHYSICA - MATHEMATICA

REDUCTION AND ANALYSIS METHODS OF INDIGO

by

Anne Vuorema

TURUN YLIOPISTO
Turku 2008

From the Department of Chemistry, University of Turku, Finland

Supervised by
Dr Marjo Keskitalo
Plant Production Research,
MTT Agrifood Research Finland, Finland.

Dr Frank Marken
Department of Chemistry,
University of Bath, UK.

Reviewed by
Professor Thomas Bechtold
Research Institute for Textile Chemistry and Textile Physics,
University of Innsbruck, Austria.

Professor Fritz Scholz
Institute of Biochemistry,
University of Greifswald, Germany.

Opponent
Professor Bernd Rudolph
FB SciTec,
University of Applied Sciences Jena, Germany.

Custos
Professor Keijo Haapakka
Department of Chemistry,
University of Turku, Finland.

ISBN 978-951-29-3781-3 (PRINT)
ISBN 978-951-29-3782-0 (PDF)
ISSN 0082-7002
Painosalama Oy – Turku, Finland 2008

CONTENTS

ABSTRACT

Throughout history indigo was derived from various plants for example Dyer's Woad (*Isatis tinctoria* L.) in Europe. In the 19th century were the synthetic dyes developed and nowadays indigo is mainly synthesized from by-products of fossil fuels. Indigo is a so-called vat dye, which means that it needs to be reduced to its water soluble *leuco*-form before dyeing. Nowadays, most of the industrial reduction is performed chemically by sodium dithionite. However, this is considered environmentally unfavourable because of waste waters contaminating degradation products. Therefore there has been interest to find new possibilities to reduce indigo. Possible alternatives for the application of dithionite as the reducing agent are biologically induced reduction and electrochemical reduction. Glucose and other reducing sugars have recently been suggested as possible environmentally friendly alternatives as reducing agents for sulphur dyes and there have also been interest in using glucose to reduce indigo. In spite of the development of several types of processes, very little is known about the mechanism and kinetics associated with the reduction of indigo. This study aims at investigating the reduction and electrochemical analysis methods of indigo and give insight on the reduction mechanism of indigo. Anthraquinone as well as it's derivative 1,8-dihydroxyanthraquinone were discovered to act as catalysts for the glucose induced reduction of indigo. Anthraquinone introduces a strong catalytic effect which is explained by invoking a molecular "wedge effect" during co-intercalation of Na^+ and anthraquinone into the layered indigo crystal.

The study includes also research on the extraction of plant-derived indigo from woad and the examination of the effect of this method to the yield and purity of indigo. The purity has been conventionally studied spectrophotometrically and a new hydrodynamic electrode system is introduced in this study. A vibrating probe is used in following electrochemically the *leuco*-indigo formation with glucose as a reducing agent.

Keywords: indigo, woad, reduction, glucose, dithionite, anthraquinone, catalysis, electrochemistry, sonoelectrochemistry

LIST OF SYMBOLS AND ABBREVIATIONS

Abbreviations

DHAQ	1,8-dihydroxyanthraquinone
NMP	N-methylpyrrolidone
SCE	Saturated calomel electrode
SEM	Scanning electron microscope
THAQ	1,8,9,10-tetrahydroxyanthracene

Symbols used in equations

A	electrode area (m^2)
c	bulk concentration (mol m^{-3})
D	diffusion coefficient (m^2 s^{-1})
δ	diffusion layer thickness (μm)
E	potential (V)
F	Faraday constant (96485 C mol^{-1})
I_{lim}	limiting current (A)
k'	chemical dissolution rate constant (m s^{-1} × mol m^{-3})
k_{app}	apparent rate constant (mol m^{-3} s^{-1})
M	molar mass (kg mol^{-1})
n	number of electrons
N_A	Avogadro's number (6.022×10^{23} mol^{-1})
N_P	number of molecules in particle
ω	rate of rotation (radian s^{-1})
π	3.14159
R	gas constant (8.314 J K^{-1} mol^{-1})
r	particle radius (μm)
ρ	density (kg m^{-3})
S	particle surface area (m^2)
t	time (s)
T	absolute temperature (K)
v	scan rate (Vs^{-1})
υ	kinematic viscosity of solution, viscosity η / density ρ (m^2 s^{-1})

LIST OF ORIGINAL PUBLICATIONS

I. Vuorema, A.; John, P.; Jenkins, A.T.A.; Marken, F. A rotating disc voltammetry study of the 1,8-dihydroxyanthraquinone mediated reduction of colloidal indigo *Journal of solid state electrochemistry,* **2006**, *10*, 865-871.

II. Vuorema, A.; John, P.; Keskitalo, M.; Kulandainathan, M. A.; Marken, F. Electrochemical and sonoelectrochemical monitoring of indigo reduction by glucose *Dyes and Pigments* **2008**, *76*, 542-549.

III. Vuorema, A.; John, P.; Keskitalo, M.; Marken F. Electrochemical Determination of Plant-Derived Leuco-Indigo after Chemical Reduction by Glucose *Journal of Applied Electrochemistry* **2008**, *38*, 1683–1690.

IV. Vuorema, A.; John, P.; Keskitalo, M.; Mahon, M.F.; Kulandainathan, M.A.; Marken, F. Anthraquinone catalysis in the glucose driven reduction of indigo to *leuco*-indigo *Physical Chemistry Chemical Physics*, in press.

V. Vuorema, A.; Ketoja, E.; Keskitalo, M. Content and purity of indigo from Dyer's Woad (*Isatis tinctoria* L.) produced in the North Europe, submitted to *Industrial Crops and Product*s.

1. INTRODUCTION

Indigo is one of the oldest dyes used by mankind. The current consumption of the dye is enormous due to the popularity of blue jeans, which are dyed with indigo. The consumption of indigo and other vat dyes reaches about 33 million kg annually [1] and the reduction of indigo to *leuco*-indigo represents an important type of industrial process which is operated worldwide on a considerable scale [2]. Throughout history indigo was derived from various plants. Dyer's Woad (*Isatis tinctoria* L.) was cultivated in wide areas in Europe until indigo from *Indigofera* species (*Indigofera tinctoria*) from India started to be imported in bigger scale in the 17th century [3]. In the 19th century came the synthetic dyes and nowadays indigo is mainly synthesized from by-products of fossil fuels. Recently there has been a growing interest in natural products obtained from renewable resources instead of oil supplies, which are non-renewable [4]. Especially woad is interesting dye plant to cultivate in Europe and it can be grown also in Finland.

Indigo is a so-called vat dye, which means that it needs to be reduced to its water soluble *leuco*-form before dyeing. The reduced form is absorbed into the fibres, and when oxidized back to its blue form it stays within the fibre [5]. Earlier the reduction and dyeing was done with fermentation [6,7]. Nowadays, the most of the reduction has been done chemically by sodium dithionite. It is considered environmentally unfavourable since it produces sulphite, sulphate, thiosulphate and toxic sulphides as degradation products, which then contaminate the waste waters from the dyeing plants [2]. Therefore there has been interest to find new possibilities to reduce indigo.

Possible alternatives for the application of dithionite as the reducing agent are bacteria induced reduction and electrochemical reduction. A gram-positive, aerobic moderate and thermophile bacteria *(Clostridium isatidis)* capable of reducing indigo dye was isolated from woad vat at the University of Reading, UK [7,8]. In the electrochemical approach the possibilities are direct [9] or indirect [10,11] electrochemical reduction with different redox mediators. Organic reducing agents have also been investigated as possible alternatives to the sodium dithionite [12]. Glucose and other reducing sugars

have recently been suggested as possible environmentally friendly alternatives as reducing agents for sulphur dyes [13] and there has also been interest in using glucose to reduce indigo [14].

In addition to reducing sugars alone as organic reducing agents, anthraquinones can assist in the glucose induced reduction of synthetic indigo in which they act as catalysts. Anthraquinones have been previously recognized to stimulate indigo reduction by pure cultures of bacteria [15,16] and anthraquinone-rich madder powder is known to have been an invariable ingredient in the medieval indigo dye vat [17]. Anthraquinones are also known to act as mediators in the indirect electrochemical reduction of indigo, where they transfer electrons between electrode and dye molecule [18].

In spite of the development of several types of processes, very little is known about the mechanism and kinetics associated with the reduction of dispersed indigo. This study aims at investigating the reduction and analysis methods of indigo and give insight on the reduction mechanism of indigo. The study includes also research on the extraction of plant-derived indigo from woad and the examination of the effect of this method to the content and purity of indigo.

2. REVIEW OF LITERATURE

This literature review consists of sections with the history of indigo and its chemistry as well as its reduction and related analysis methods. The aim of this review is to give a concise background of indigo and its reduction methods.

2.1. HISTORY OF INDIGO

Indigo has been used for thousands of years, and it's one of the oldest dyes used by mankind. There is evidence of indigo being used already in mummy cloths in ancient Egypt [4,19]. Before the synthetic dyes were developed in the 19th century indigo as well as other dyes were produced from plants [20]. In Europe, Dyer's Woad (*Isatis tinctoria* L.) was cultivated for indigo production and *Indigofera* species (for example *Indigofera tinctoria*) were used in the tropics. Dyer's knotweed (*Polygonum tinctorium*) was cultivated for indigo in China and Japan. Woad is a temperate herbaceous biennial plant and it produces leaf rosettes on the first year (see Figure 1), which are harvested for the indigo production and on second year it produces flower stems and seeds for reproduction [21]. Woad is native to South-East Russia and it has spread from there to cultivation in the rest of Europe [17]. Woad was an important crop in Europe in the middle ages and it brought immense wealth to the woad traders. The renowned centres of the trade were Toulouse in France and Erfurt in Germany which still have some lingering effect of woad commerce [19].

Figure 1. First year leaf rosette of woad (*Isatis tinctoria* L.) grown in Jokioinen, Finland (60°49'N, 23°29'E).

The tropical indigo overtook European markets in the 17th century even if the woad traders did all in their power to stop that. The indigo produced in India and Java replaced woad in such a way that the woad cultivation was diminished until it disappeared entirely in the beginning of the 20th century with the appearance of synthetic indigo to the markets. Synthetic indigo destroyed almost completely the production of tropical indigo as well [4,19]. The synthetic dyes brought also other blue dyes and these had superior qualities when compared to indigo and this would have ruined the synthetic indigo as well if the jeans hadn't begun their invasion to the western culture after second world war [19]. Lately, there has been new demand on finding alternatives for the products made from the non-renewable materials, such as oil based dyes, and there is an on-going research on developing methods to produce biologically manufactured indigo.

2.2. PRODUCTION OF INDIGO

The structure of indigo was first suggested by von Bayer in 1869 and the first commercially successful synthesis of indigo was based on the process published by Heumann in 1890 [3,22]. The BASF started the production in 1897 [23]. This synthetic process converted phenylglycine-o-carboxylic acid by fusion with sodium hydroxide into indigo via indoxyl-2-carboxylic acid [24]. Indigo production with hydrocarbon degrading bacteria expressing mono-oxygenases or dioxygenases have also been investigated in search of a possible alternative for the chemical synthesis of indigo [25,26]. For example, Berry *et al*. [27] developed a fermentation process where indigo was produced from glucose with recombinant *Escherichia coli* which had been modified with *Pseudomonas putida* genes. However the method produced also indirubin which gave undesirable red hue to the dyeing result which they were able to suppress to a point [28].

In the traditional method of producing indigo dye (also called woad) from woad, the leaves were crushed to pulp which was kneaded into balls, which were allowed to dry for several weeks. These dried balls could then be stored. The balls needed to be couched before they could be used in dyeing. The couching meant crushing the balls

into powder and wetting it and allowing the material to ferment for several weeks again. After couching, the woad was dark clay-like material which was dried and packed tightly before use [17,29].

The dye from woad was very impure and it gave only light colours and this was the reason why the exotic indigo from the *Indigofera* species could overtake woad so completely. The indigo from tropics was a better quality and it could be used to produce darker blues. However even this was still impure and was substituted by the synthetic indigo which always produced purities over 90% [20]. The extraction from the *Indigofera* was done differently from the woad extraction. The plant material was steeped with water (fermentation) and after that the solution was oxidised with air [30]. The modern extraction method of indigo from woad follows a similar method, and the woad balls are no longer made.

Indigo itself doesn't exist in the leaves of indigo producing plants. Instead there are its precursors, indican in *Indigofera* species and *Polygonum tinctorium* [31] and isatan B in addition of indican in *Isatis tinctoria* [19]. Lately there have been suggestions of other precursors being present in woad as well, namely isatan A [32,33] and isatan C [34]. There have also been some questions on their structures. Indican has been identified as indoxyl-β-D-glucoside but the already established isatan B structure as indoxyl-5-ketogluconate [35,36] was questioned by Oberthür *et al*. [32] and they suggested it to be 1*H*-indol-3-yl *β*-D-ribohex-3'-ulopyranoside. They also gave isatan A a structure as 1*H*-indol-3-yl 6'-O-(carboxyacetyl)-*β*-D-ribohex-3'-ulopyranoside whereas Maugard *et al*. [34] didn't give specific structure for the isatan C.

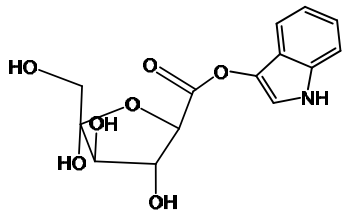

Indoxyl-5-ketogluconate = isatan B

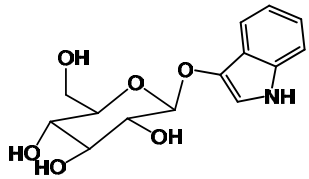

Indoxyl-B-D-glucoside = indican

Scheme 1. The molecular formulas of the precursors of indigo.

Free indoxyl has been suggested to form indigo by indoxyl radical which first forms *leuco*-indigo which is then oxidised to indigo [37]. The *leuco*-indigo being the reduced form of indigo, which is later needed in the dyeing process because of its solubility in water, whereas indigo itself is not soluble in water or other commonly used solvents [3]. The modern extraction method of indigo from woad uses the water solubility of the indigo precursors in steeping the leaves in hot water. The precursors are broken down to indoxyl and sugar moieties by enzymes in plant, but in the extraction method this is done by alkali with aeration [38,39,40,41].

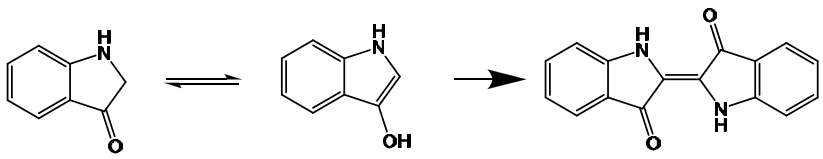

Scheme 2. The molecular formulas of indoxyl and indigo.

The purity of plant-derived indigo even with the modern extraction method is somewhat low when compared to the synthetic indigo. Natural indigo contains besides indigo, impurities such as indirubin, indigo-brown, indigo gluten and mineral matter [42,43]. The indigo purity has been reported to be for woad indigo 20-40% [38], for *P. tinctorium* up to 12% [44] and for *Indigofera* indigo the highest from 50 up to 77% [30]. There is also the question of the efficiency of the extraction, the theoretical yield of the indigo formation from indoxyl molecules have been discovered to be approximately 60% [20]. So 40% of the indoxyl is lost during the process to impurities such as isatin and indirubin and other by-products of the reaction.

2.3. PROPERTIES OF INDIGO

The indigo which is also known as indigotin, (CI Vat Blue 1), (2-(1,3-dihydro-3-oxo-2*H*-indol-2-ylidene)-1,2-dihydro-3*H*-indol-3-one) is present at ambient temperature and normal pressure as dark blue-violet needles or prisms with distinct coppery lustre [45,46]. It is quasiplanar molecule of approximate dimensions of 4.8×12 Å [47]. Indigo crystallises monoclinic and in space group $P2_1/C$ [48]. It sublimes above 170 ºC [49]. Indigo is insoluble in water and poorly soluble in most of the common solvents [3]. It

is more soluble in polar organic solvents than non-polar ones [49,50]. The poor solubility is most likely due to the strong inter- and intramolecular hydrogen bonds that are formed in indigo crystals [51]. The hydrogen bonding also explains indigo's relatively high melting point (~390 ºC) as well as its bathocromic shift of colour [24]. The colour of indigo is dependent on its environment [52]. In the gas phase where indigo is in its monomeric form, it is red, and in nonpolar solvents it is violet, but in solid form and in polar solvents as well as when it is applied to textiles as a vat dye, it is blue [53]. Indigo has a low mammalian toxicity and there is no indication of sensitization in humans after repeated skin applications [49].

Indigo is classified as a vat dye although its properties are not typical to the vat dyes as a whole [54]. Indigo has been mentioned to have a moderate [24] to very high light-fastness [55] depending on the substrate it is on or whether it is as a pigment or a dye. All in all, it's among the most photo-stable natural dyes. The light mostly affects the oxidative degradation of indigo to the degradation products such as isatin, isatoic anhydride and anthranilic acid [55]. There are synthetic dyes especially vat dyes with better fastness properties particularly to light, washing and chlorine bleaching, than indigo but it is this fading of colour that is so characteristic of indigo that has kept it so popular with the jeans-wearing people [54,56].

2.4. REDUCTION OF INDIGO

As a vat dye indigo needs to be reduced to its water-soluble form before it can be used in dyeing. The reduction of indigo to *leuco*-indigo represents an important type of industrial process which is operated worldwide on a considerable scale [2]. The vat dyes have a conjugated dicarbonyl system, which is reduced with a change in conjugation. The reduction is a two-electron change and the resulting dihydric alcohol can be easily reoxidised [57,58]. The reduced form is called the *leuco* compound, *leuco* coming from the Greek word *leucos* meaning white, which refers to the change of colour of the vatting liquid after reduction [45]. With indigo the colour of the *leuco*-indigo solution is yellow green when reduced with sodium dithionite.

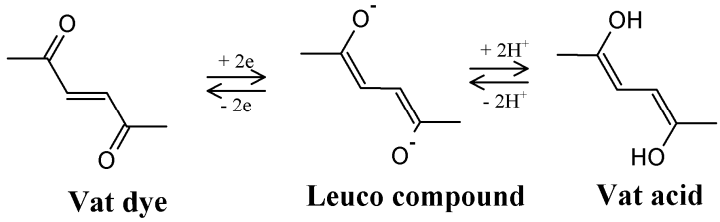

Scheme 3. The reduction process of the conjugated dicarbonyl system of vat dyes.

Depending on the dyebath pH the vat dye can undergo two-step ionisation from the non-ionic form to either mono-ionic or di-ionic, the non-ionic form being called vat acid [57,59]. For indigo the pK_a-values have been determined to be for pK_1 8.0 and for pK_2 12.7 [59]. The extent of ionisation has an effect on the affinity of indigo for cotton cellulose fibres which are the most common substrate for indigo due to the popularity of denim. Indigo as well as cellulose fibres are negatively ionised at high pH. Cellulose contains alcoholic OH-groups which begin to be deprotonated when the dyebath pH is increased to 11, above which the deprotonation occurs more strongly. The non-ionic form of indigo at lower pH is poorly soluble in the dyebath as well as it has a poor substantivity towards the cellulose fibres. Whereas the di-ionic form has high solubility but poor substantivity. The mono-ionic form has been identified to be the most efficient form of indigo and it predominates within the pH range of 10.8-11.2 [60]. So the equilibrium sorption of indigo for cotton is at its highest at a dyebath of pH around 11 [61,62].

Several different methods have been invented for the indigo reduction and dyeing, all starting from the fermentation vat, which was used for centuries before the modern technology came. The fermentation process was done in large wooden barrels called vats from which the name for the vat dyes also comes. There were also urine vats which used stale urine as an ingredient in the fermentation. The industrial revolution brought new possibilities to the dyeing with such methods as “copperas” method which combined ferrous sulphate with slaked lime or potash and zinc-lime vat in which slaked lime and zinc powder interacted to form hydrogen as a reducing agent. The universal reducing agent sodium dithionite was finally introduced to the vat dyeing at the end of the 19th century [19].

2.4.1. Sodium dithionite

Sodium dithionite also known as sodium hydrosulphite, or Hydro ($Na_2S_2O_4$) has been a major reducing agent [63] in the industrial reduction of vat dyes including indigo due to its chemical as well as economic properties. It is used with all vat dyes at temperatures ranging up from 30 °C [64]. It is generally produced by the zinc dust and the "amalgam" processes [65]. The advantage with sodium dithionite is that it causes swift reduction of indigo as well as other vat dyes and it enables very short fixing times in various dyeing methods and produces levelness in continuous dyeings [45].

However, the disadvantage of sodium dithionite is that it can not be recycled from the waste waters and used again in the reduction process [66]. It is unstable, it is very easily oxidised by atmospheric oxygen [67] and the stability of its alkaline solutions reduces with the increase of temperature even in the absence of oxygen. The result is that large amounts of dithionite and NaOH are needed over the stoichiometric requirements of the reduction process although there has been speculation on whether the amount of dithionite could be lowered and used more efficiently [68]. The oxidation byproducts cause various problems with the disposal of waste waters. The generation of sulphate (SO_4^{2-}), sulphite (SO_3^{2-}), and thiosulphate ions ($S_2O_3^{2-}$) have harmful effect on the environment due to their toxicity as well as their having a corrosive effect on the waste lines. In addition sodium dithionite affects the aerobic processes in the water treatment and toxic hydrogen sulphide [H_2S] can form anaerobically from the sulphate deposits present in the waste waters [45,64]. To improve this type of process by eliminating or minimizing the production of inorganic waste from chemical reducing agents, alternatives such as the iron (II) complexes (gluconic acid complexes) [69], the organic reducing agents [70], borohydride [71], and the biological [7], as well as the electrochemical reduction of indigo have been proposed [1]. Also pre-reduced indigo has been introduced to the dye-houses where the *leuco*-indigo is produced by reduction via a catalytic hydrogenation process [72].

2.4.2. Biological reduction

Before modern reduction methods were invented indigo was dyed with a fermentation vat where it was converted to *leuco*-indigo by reducing bacteria [73]. Hurry [17] considered that the bacteria present in the vat were *Desmobacterium hydrogeniferum* which would also be involved with the reduction but Padden *et al.* [74] isolated an anaerobic moderate thermophile from a woad vat and they named the bacteria as *Clostridium isatidis*. The woad vat was prepared with medieval method from couched woad. The isolated bacteria grew in nutrient-rich medium at optimum temperature 49-52 ºC and at optimum pH 7.2, the pH was changed to 9 for the indigo reduction to occur [16]. Anthraquinone rich madder was added to the woad vat already in the medieval times [17]. Nicholson and John [16] studied the effect of the madder powder and anthraquinone-2,6-disulphonate and humic acid on the reduction of indigo. They all were found to stimulate the bacterial reduction of indigo and it was speculated that it was due to their ability to alter the surface properties of the bacteria or indigo [16].

To identify the mechanism of the reduction of indigo by bacteria Compton *et al.* [75] colonised carbon electrodes with *C. isatidis* and measured electrochemically the process and identified that the bacteria interacted directly with indigo particles without the redox mediator. However, John [76] questioned this later, because Gram-positive bacteria such as *Clostridium isatidis* are not known to have a biochemical mechanism which would enable the transfer of electrons from the interior of the cell to the solid electron acceptor external of the cell. So the mechanism of the bacterial reduction of indigo still remains unknown.

Enzymatic technologies using dehydrogenases have also been investigated for the reduction of vat dyes in general. However, there is no enzymatic process at present that could be used as an alternative for the chemical reduction of indigo [45].

2.4.3. Electrochemical reduction

In recent years several novel electrochemical processes have been developed for the indigo reduction and its analysis. The solid-state electrochemical properties of indigo,

the effects of pH, electrolyte, and convection have been investigated when indigo has been firmly immobilized onto a graphite electrode surface [77]. The redox properties of indigo have also been studied when small amount of indigo has been adsorbed on the surface of mercury electrode [78]. Direct electrochemical reduction of dispersed indigo for the dyeing process is somewhat complicated due to the electron transfer difficulties between solid electrode and solid particle of dye and therefore indirect electrochemical methods have been suggested first.

In this indirect method the reducing power of cathode is transferred to the solution to a soluble reversible redox system that acts as a mediator and carries the electrons from the electrode to the dye [79]. Fe(III) -triethanolamine (TEA) complex, -bicine and HEDTA iron complexes and Fe^{3+}-D-gluconate or Ca^{2+}-Fe^{3+}-D-gluconate complexes and anthraquinone derivatives have been investigated as mediators in the electrochemical reduction of indigo [18,80,81,82,83,84]. The reduction rate has been found out to depend on the type of mediator system and the type of dyestuff [85]. The general reaction scheme of the indirect electrochemical reduction of indigo and other vat dyes with iron complexes can be represented as follows [83,86]:

$$Fe^{3+}L + e^- \rightleftarrows Fe^{2+}L \quad (1)$$

$$Fe^{2+}L + Dye \rightleftarrows Fe^{3+}L + Dye^{\bullet -} \quad (2)$$

$$2\ Dye^{\bullet -} \rightleftarrows Dye^{2-} + Dye \quad (3)$$

$$Dye^{\bullet -} + Fe^{2+}L \rightleftarrows Dye^{2-} + Fe^{3+}L \quad (4)$$

$$Dye^{2-} \rightleftarrows Dye + 2e^- \quad (5)$$

The first step shows the cathodic reduction of the iron complex, the second is suggested to be a radical formation of the dye at the surface of the dye particle by electron transfer since the dye requires a two electron reduction and the complex carries only one. The fully reduced form of the dye is produced through the radical phase either by additional reaction with the complex or another radical anion. The final step shows the equilibrium between the reduced and oxidised forms of the dye [83].

The scheme can be used also for other mediator systems used in the indirect reduction of indigo.

The general requirements of the mediator in the indigo reduction are that it has sufficient negative formal potential in the alkaline solutions, at least -600 mV *vs*. Ag | AgCl | 3 mol dm^{-3} KCl to reduce the dyestuff and it has a reducible charge transfer and a high rate of electron transfer from cathode to the complex and from mediator to the dyestuff [83]. The achievable current density of the mediator process is limited by the diffusion transport of the mediators through the boundary layer of the cathode. Increasing the concentration of the mediator indefinitely and thereby increasing the current density is not feasible due to the economical and ecological considerations as well as possible changes in the product quality [87]. Multicathode cell, where the cathode material used is stainless steel, has been suggested as a possible solution to the problem of low cell current density. In this type of cell several three-dimensional cathodes are connected to a common anode and they produce the necessary high electrode surface area for the process [88].

However, the mediators in the indirect reduction system can be problematic and so there has been interest in developing another electrochemical process. The direct electrochemical reduction of indigo represents an alternative mediator-free approach. The first method for the direct electrochemical reduction of indigo introduced the mechanism in which the indigo radical is first formed in a comproportionation reaction between the *leuco*-indigo and oxidised indigo and the radical is reduced electrochemically to *leuco*-indigo. However, this method still needs the conventional reducing agent to produce the necessary *leuco*-dye to start the reaction after which it continues independently and it is not very efficient due to the low amount of radicals formed during the process [5,12,89].

Another method of the direct electrochemical reduction investigated by Roessler *et al*. [90] is electrocatalytic hydrogenation. Water is reduced electrochemically in the process to produce hydrogen which is adsorbed on the metal powder catalyst surface and reacts chemically with an organic substrate, in this case indigo or other vat dye to

produce *leuco*-dye. The electrocatalytic hydrogenation doesn't need elevated temperatures or pressures and that is a clear advantage when compared to the conventional hydrogenation [91]. The catalytic material acts as an electrode and the catalyst for the hydrogenation in the system and the Raney Nickel was considered the best option due to its availability, costs and its stability in alkaline medium. However, its current efficiency is low, and there is a limiting factor in the competing reaction of the adsorbed hydrogen forming molecular hydrogen [46].

The third alternative for the direct electrochemical reduction developed by Roessler *et al.*[9] was the electrochemical reduction of indigo in fixed or fluidized beds of graphite granules. The limiting factor in the direct reduction of indigo seems to be the poor contact between the electrode surface and the indigo particle and this was improved by the introduction of the bed of graphite granules, which would act as an electrode. Also the dispersion and adsorption of dye particles has been noticed to be important in the process. *Leuco*-indigo is produced in this system directly from the indigo and not via the radical formation, at least the radical formation is not considered to be significant in this case [2].

2.4.4. Glucose and catalysts

Hurry [17] already suggested that the organic substances added to the woad vat were fermented to glucose which acted as a reducing agent in the alkaline liquor and converted indigo to *leuco*-indigo at the same time as the sugar is oxidised and converted to lactic and then to butyric acid. When the fermentation vat was replaced by the chemical reducing agents also glucose was removed from the indigo vats.

Glucose has been known to be a reducing agent for sulphur dyes for quite some time, but it was considered to give unsatisfactory results since it was dependent on high temperatures. This was improved by having strongly alkaline conditions in the dyeing vats [70]. Recently glucose and other reducing sugars have been studied as possible environmentally friendly reducing agents for sulphur dyes but no mechanistic detail is suggested there [13]. Glucose undergoes a complex degradation sequence in alkaline solutions [92,93,94] and the reducing effect of glucose has been suggested to be linked

to the degradation intermediate rather than to glucose itself [95] where the dehydrated intermediates, of the degradation steps, with extended π-systems are most likely the redox active reducing agents. The course of degradation of glucose depends on the concentration of alkali [96,97,98] so the concentration of specific intermediate is dependent on the concentration of alkali. This explains why the high alkalinity has been deemed necessary for the reduction processes

Anthraquinone-containing madder extracts were invariably added to the fermentation vat in the middle ages, and it has been shown with pure cultures of the indigo-reducing bacterium *Clostridium isatidis*, that soluble anthraquinones stimulate bacterial indigo reduction [15,16]. Anthraquinones are vat dyes and they can be electrochemically reduced in aqueous alkaline solution at a potential similar to that for the reduction of indigo, forming the two-electron two-proton anthraquinol product, which subsequently transfers electrons to the suspended indigo. Therefore the anthraquinones have also been examined in the electrochemical indirect processes as soluble mediators [18] and immobilised on the graphite granules to stimulate the direct reduction of indigo on graphite beds [9].

2.5. METHODS OF INDIGO ANALYSIS

Indigo production as well as dyeing processes need means to measure the indigo content. In the indigo production from plants the final dye content varies from batch to batch and the purity of the raw dye needs to be determined separately. In the dyeing the monitoring of the vatting process is necessary so that the dyeing quality can be maintained stable.

The colorimetric monitoring of solid indigo dye presents some technical problems [20]. Indigo is routinely determined by spectrophotometry of solutions using a variety of organic solvents [8,29,99]. Indigo has also been determined spectrophotometrically by first reducing it to its soluble *leuco*-form and measuring the absorbance of the reduced alkaline aqueous solution, this has been especially used in the dyeing processes [44,100]. Also recently the absorption of the reoxidised indigo has been used to quantify the concentration of indigo in the vatting solution [101]. It has been pointed

out that these methods that directly measure indigo concentration are subject to anomalies due to the long recognized association of indigo molecules in the solvents that are routinely employed in the measurements [20,51]. Also other particles present in the solutions, such as the impurities present in the natural indigo and the auxiliary agents in the vatting system, can affect measurements.

Since vat dyes are redox active, electrochemical measurements are possible and have been studied for vat dyes [102], including indigo [103,104] as well as for their reducing agent, sodium dithionite [105] mainly to control the stability of the dyeing vats and to improve the product quality. With the electrochemical methods the disturbancies to the measurements from the other particles present in the vat can be lowered. There has been interest in developing these methods for a continuous use, however there has been only a limited success in that since the electrode surfaces as well as valves or pumps of the system are easily blocked by the oxidised dyestuff [104].

Some of the methods use redox titrimetry, where *leuco*-indigo is titrated with the oxidising agents such as potassium ferrocyanide and the redox potential is measured from the mixture until the potential is zero, which denotes the end of the reaction and the amount of *leuco*-indigo is obtained [100]. Other methods use hydrodynamic voltammetry to measure the indigo content [103,105].

Hydrodynamic voltammetry provides time independent steady-state responses, which, under conditions of mass transport control, are directly proportional to the bulk concentration. Hydrodynamic concentration monitoring techniques have been based on, for example, rotating disc voltammetry [103], jet voltammetry [106], microwave enhanced voltammetry [107], sonovoltammetry [108], and vibrating electrode systems [109]. Govaert *et al*. have employed the rotating disc voltammetry [103] to measure the indigo content, they used a multi-pulse amperometric technique to produce a semi-continuous measurement of indigo where the pulses to negative potentials were necessary to clean the electrode surface from the adsorbed dyestuff.

3. AIMS OF THE STUDY

This study aims at investigating the reduction and analysis methods of indigo and give insight on the reduction mechanism of indigo employing synthetic indigo as research material. The study includes also research on the extraction of plant-derived indigo from woad and the examination of the effect of this method to the content and purity of indigo. The results of this study may be used as a basis for further investigation of the reduction of plant-derived indigo and development of more sustainable dyeing method of synthetic as well as plant-derived indigo.

The aims of the study were to:

- quantify the mediator-based electrochemical reduction of dispersed indigo when DHAQ is used as a redox mediator.

- investigate the possible reducing effect of glucose on indigo quantitatively to develop an alternative reduction method for indigo.

- investigate the catalytic effect of anthraquinones on the glucose assisted reduction of indigo and to propose a possible molecular mechanism of the catalytic effect on the indigo reduction.

- develop a new sonoelectrochemical method for determination of indigo reduction and quantifying the indigo/*leuco*-indigo concentration in the solution.

- gain new insight into the extraction method of plant-derived indigo and measurement of the purity of indigo with the sonoelectrochemical method.

4. EXPERIMENTAL

4.1. REAGENTS (I-IV)

Chemical reagents such as indigo (Fluka), phosphoric acid, sodium hydroxide (Aldrich), acetone, anthraquinone, butylated hydroxyl toluene, D-(+)-glucose, N-methylpyrrolidone (Sigma), potassium ferrocyanide, 1,8-dihydroxyanthraquinone (Sigma-Aldrich), hydrochloric acid and calcium hydroxide (J.T.Baker) were obtained commercially and used without further purification in the experiments. Demineralised water was taken from an Elga purification system with at least 15 MOhm cm resistivity. Argon gas was used for de-aeration and obtained from BOC.

4.2. PLANT-DERIVED INDIGO SAMPLES (III,V)

Plant-derived indigo samples were from the extraction experiment conducted in MTT Agrifood Research Finland in summer 2004. Indigo was extracted from Dyer's woad (*Isatis tinctoria* L.) leaves with the method shown below. Woad plants were grown in Jokioinen, Finland (60°49'N, 23°29'E) in summer 2004, the seeds were sown in green house on 7th May 2004 and the plants were transplanted to the field after 4 weeks from sowing and they had been grown for 5 weeks in field at the beginning of the experiments. All the leaves in the samples were collected on the day they were used in the extraction and they were chosen randomly from the plot from the close proximity of each other. The leaves were approximately the same size within a batch, although there were variations in the leaf size between batches.

4.2.1. The Extraction method of indigo (IV,V)

The extraction method used in the experiment was based on the protocol by Stoker and Cooke [38] with modifications. Woad leaves were first washed and then 50 g of leaves was put in 500 ml of 80 °C deionised water water for about 8 min after which the leaves were taken off and the water was cooled quickly to room temperature. The pH of the samples was changed to 11 by adding saturated calcium hydroxide (50 g dm^{-3}) after that the suspension was aerated for 1 h with pressurized air, after which the sample was covered and put to storage. The next day concentrated hydrochloric acid

was added and the pH was lowered under pH 4. After 2 hours, an aliquot was taken to the analysis of the indigo content. Rest of the indigo was dried. Different treatments of the extractions were studied according to the Table 1.

Table 1. Extraction process divided with extraction steps showing the standard treatments and the studied treatments for each step. Standard treatments being the ones used generally in the extraction.

Extraction steps	Standard treatments	Studied treatments
Washing times	3	0, 1, 2, 4, 6, 8, 10
Steeping		
temperature	80 °C	RT, 80 °C
time at 80 °C	8 min	4, 6, 8, 10, 12 min
pH	water	3, 5, water, 7, 9
Cooling time	<2 min	<2, 5, 10, 15, >40 min
Aeration		
time	60 min	5, 15, 45, 60 min
pH	11	7, 9, 11, 13

4.3. INSTRUMENTATION (I-IV)

All electrochemical experiments were conducted with a micro-Autolab II potentiostat system (EcoChemie, Netherlands) equipped with a three-electrode system, where a Pt wire or Pt mesh acted as a counter electrode and a saturated calomel electrode (SCE) as a reference electrode (Radiometer, Copenhagen). Working electrode varied depending on the experiment. All of the voltammetric experiments were conducted in a thermostated electrochemical cell (with a Haake B3 circulator) under constant de-aeration with high purity argon and at the constant temperature. Schematic drawing of the system for rotating disc experiments is shown in the Figure 2.

4.4. SOLID STATE ELECTROCHEMISTRY (I,IV)

Synthetic indigo or anthraquinone was immobilised on a 4.9 mm diameter basal plane pyrolytic graphite electrode, which was used as a working electrode [110,111,112]. Depending on the experiment either 0.1 M phosphate buffer (at pH 7 and at pH 12)

was thermostatted to room temperature or to 80°C or 0.1M NaOH was thermostated to RT, 55, 65, or 75 °C. The cyclic voltammograms were measured at different scan rates.

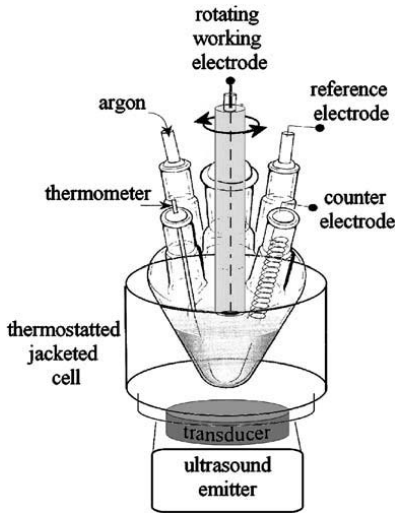

Figure 2. Schematic drawing of the thermostatted electrochemical cell for rotating disc voltammetry experiments.

4.5. HYDRODYNAMIC PROCESSES (I-IV)

4.5.1. Indirect electrochemical reduction of indigo (I)

Electrochemical reduction of indigo was mediated with 1,8-dihydroxyanthraquinone. A 7 mm diameter rotating gold disc electrode was used as the working electrode. The home-build electrochemical cell was thermostated and equipped with an ultrasonic transducer (Undatim, 100 W, 500 kHz) to minimize sedimentation effects. Indigo dispersions were prepared by treatment with 24 kHz ultrasound. Control experiments in the presence and in the absence of 500 kHz ultrasound were recorded to avoid direct effects of ultrasound on the electrochemical process. Only at a rate of electrode rotation lower than 1 Hz additional ultrasonic mass transport effects were observed. Most of the experiments were conducted at 80 °C.

4.5.2. Simulation of indirect reduction processes of indigo (I)

For quantitative data analysis, cathodic limiting currents obtained at various electrode rotation rates and reagent concentrations were employed. A commercially available

numerical simulation Digisim software package (Digisim3, Cyclic voltammetric simulator for Windows, version 3.03, BASi, USA [113]) allows rotating disc voltammograms to be simulated based on the appropriate temperature, T = 353 K, the viscosity, η = 0.0035 cP, the diffusion coefficient (for the redox mediator DHAQ, D = 0.84×10^{-9} m^2 s^{-1}), the concentrations, and further chemical parameters. For the mechanism a simple two-electron transfer followed by a chemical reaction step was chosen assuming that the dispersed particles are small enough to be approximately represented by a homogeneous concentration parameter. The additional effects of dispersed particles on the mass transport at electrode surfaces described in the literature, for example, for $CaCO_3$ particles [114], are concentration dependent. Test experiments with indigo solutions and inert redox couples revealed no significant effect under conditions employed here, and therefore, these effects are not further considered.

4.5.3. Glucose assisted reduction of indigo (II)

A 3 mm diameter glassy carbon disc electrode (BAS, USA) was used as the working electrode with glucose acting as a reducing agent in rotating disc and sonovoltammetric experiments. The latter were conducted in an inverted voltammetric cell and employing a Hielscher UP200s 24 kHz ultrasonic glass probe system.

4.5.3.1. Rotating disc procedure (II)

A NaOH solution was thermostated to needed temperature and indigo added after dispersion in a small volume of solution by treatment with 24 kHz ultrasound. Glucose was added and voltammograms were recorded as a function of time. The rotation speed in all experiments was 5.0 Hz and the mass transport controlled limiting current (which is directly proportional to concentration) was measured for the *leuco*-indigo oxidation process.

4.5.3.2. Power ultrasound procedure (II)

An inverted cell shown in the Figure 3 [115] with the working electrode pointing up towards an ultrasonic horn probe (24 kHz) was employed to measure mass transport limited currents for the *leuco*-indigo oxidation. Otherwise, the procedure is consistent

with that used for rotating disc voltammetry monitoring of the *leuco*-indigo concentration.

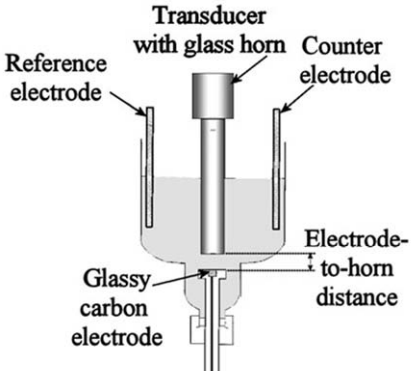

Figure 3. Schematic drawing of the experimental set up employing an ultrasonic horn system placed opposite to the glassy carbon working electrode.

4.5.4. Sonic electrode (III, IV)

New equipment was introduced in the experiments where a vibrating 500 µm diameter gold disc electrode acted as the working electrode. The electrode was embedded in a home-build PEEK (Polyetheretherketone) probe and connected to a sonic probe (Braun, Oral-B Sonic Complete) to produce a sonic vibration with approximately 1000 µm amplitude at high power or ca. 200 µm amplitude at low power (see Figure 4). The vibration frequency 250 Hz was determined optically with photodiode connected to an oscilloscope.

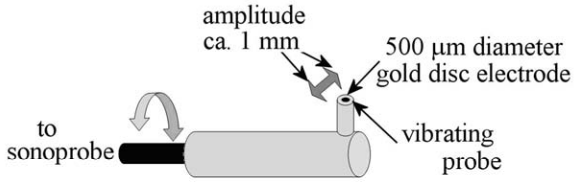

Figure 4. Schematic drawing of the sonoprobe design with a 500 µm diameter gold electrode embedded in a PEEK housing undergoing a 250 Hz lateral movement with ca. 1000 µm amplitude (high power) or ca. 200 µm amplitude (low power).

4.5.4.1. Calibration of the sonic electrode (III)

A solution of 2.4 mM $K_4Fe(CN)_6$ in 0.1 M KCl was thermostated to 55, 65, or 75 °C in a jacketed three electrode electrochemical cell. Cyclic voltammograms were recorded with a scan rate ranging from 0.1 to 5.0 V s^{-1}. In the absence of agitation, conventional

voltammetric responses were obtained which allowed the diffusion coefficient to be assessed as a function of temperature. Next, the vibrating electrode was activated and voltammograms obtained at high/low power setting to assess the mass transport effect under these conditions as a function of temperature.

4.5.4.2. The Sonovoltammetric determination of indigo (III,IV)

An aqueous 0.2 M NaOH solution was thermostated to 55, 65, or 75 °C, and plant-derived indigo was added after dispersion in a small volume of solution in a sonic bath. Next, glucose was added, and voltammograms were recorded at regular time intervals. From the limiting currents observed for the oxidation of *leuco*-indigo the concentration of indigo was determined and at the endpoint of the reduction process the total amount of indigo in the sample was calculated.

4.5.4.3. Anthraquinone catalysed reduction of indigo (IV)

Anthraquinone catalyst was immobilised onto indigo particles by adding an acetone solution (concentration 0.3 mM) to solid indigo powder. The suspension was homogenised with 24 kHz ultrasound (Hielscher UP200G) and the acetone solvent was evaporated to leave anthraquinone coated onto the indigo powder. An aqueous NaOH solution (100 cm^3) was thermostated to 55, 65, or 75 °C and 30 mg indigo added (corresponding to 1.1 mM solution) after pre-dispersion in a small volume of solution by treatment with 24 kHz ultrasound. Next, 400 mg glucose (corresponding to 22 mM solution in 100 cm^3 of NaOH) was added under an atmosphere of argon and voltammograms (limiting currents for the oxidation of *leuco*-indigo) at the vibrating gold disc electrode were recorded at regular time intervals. Polishing the gold electrode surface before each measurement was required.

4.6. INDIGO SUBLIMATION AND SEM (IV)

Indigo crystals were formed following sublimation in a short path vacuum sublimation system (made from glass) with internal water-cooled deposition finger. The system was heated in silicone oil to a temperature of ~240 °C. Sublimation under oil pump vacuum (ca. 10^{-3} Torr) was continued for 3 days (nights excluded). Macroscopic but very thin plate-like indigo crystals were obtained. Indigo crystals were collected and attached to

the double-sided conducting carbon sticky pads for SEM, which were mounted on glass slides. The glass slide with indigo crystal samples were immersed in the reduction solution (33 mM glucose in 0.2 M NaOH at 65 °C). Samples of indigo, exposed to reducing conditions for different lengths of time, were rinsed in water, dried, and used directly for electron microscopy (after gold sputter coating). Scanning electron microscopy (SEM) images were obtained with a JEOL JSM6310 system.

4.7. SPECTROPHOTOMETRIC DETERMINATION (IV,V)

4.7.1. Ethyl acetate method (V)

The indigo content of the extraction suspension was determined spectrophotometrically [38,116]. An aliquot was taken from the extraction and diluted with deionised water, added ethyl acetate to transfer indigo from the suspension to the solvent layer. Separated the layers and added NaCl to the ethyl acetate phase to remove the moistness, the samples were centrifuged. Indigo content was measured from the ethyl acetate phase at 600 nm with spectrophotometer (UV-160A UV-visible recording spectrophotometer, Shimadzu). The indigo content was determined with calibration curve measured with synthetic indigo.

4.7.2. NMP method (V)

Spectrophotometric determination of the indigo purity was attempted following a modified literature method for measuring the indigo content in the raw sample [20,116,117]. A blue solution was prepared by dissolving dried indigo samples into 90% N-methylpyrrolidone (NMP) (wet, with 0.1% butylated hydroxyl toluene and 3 mM citric acid). The absorbance of the solution was measured at a peak at 614 nm with a UV-160A UV-Visible spectrophotometer (Shimadzu). The indigo content was determined from the absorbance with the calibration curve measured with synthetic indigo.

5. RESULTS AND DISCUSSION

5.1. SOLID STATE ELECTROCHEMISTRY (I,IV)

It has been shown previously that solid indigo immobilized at a graphite electrode can be studied directly by electrochemical methods [77]. The microcrystalline solid is embedded in the electrode surface, and both reversible reduction and oxidation processes are observed. These processes are temperature as well as pH dependent [118]. The temperature dependence of these processes is shown in the Figure 5 (A). Cyclic voltammograms were obtained for the reduction of solid indigo immobilized at a basal plane pyrolytic graphite electrode and immersed in 0.1 M phosphate buffer (at pH 7 and at pH 12, results not shown) or aqueous 0.1 M NaOH (pH 13).

The two redox processes, P1 at -0.75 V *vs*. SCE and P2 at -0.1 V *vs*. SCE, have been proposed to be consistent with mechanisms given in equation (6) [77]. The reduction process P1 is associated with the electron transfer and deprotonation of indigo. Depending on the pH indigo is in non-ionic, anionic or dianionic form. At higher pH the reduction process P1 is also associated to an intercalation process involving the Na^+ cation which ultimately causes the break-up of the indigo solid during reductive dissolution (pK_2 12.7 [59]) [77]. At pH 13 these two processes, based on H^+ and Na^+, merge into a single reductive dissolution response, but even then the dissolution of indigo remains rate-limited by the relatively slow dissolution process and the removal of indigo away from the electrode occurs. The process P2 is associated with the oxidation of indigo.

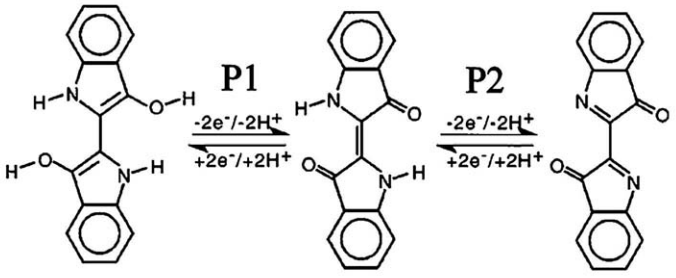

(6)

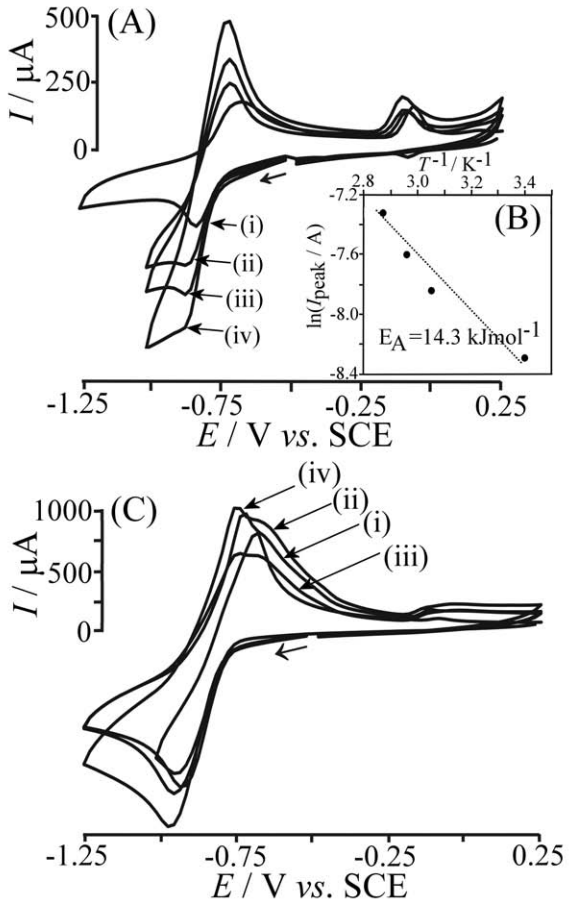

Figure 5. Solid state voltammetry data (scan rate 0.2 V s^{-1}) (A) for the reduction of indigo microcrystals and (C) for the reduction of anthraquinone microcrystals immobilised at a basal plane pyrolytic graphite electrode and immersed in aqueous 0.1 M NaOH. Data were obtained at temperatures (i) 20 °C, (ii) 55 °C, (iii) 65 °C, and (iv) 75 °C with starting potential -0.5 V. (B) Arrhenius plot of the indigo reduction peak current versus T^{-1}.

The voltammograms shown in the Figure 5 (A) were obtained at 20, 55, 65, and 75 °C. The cathodic current response increases with temperature and this suggests that the rate of the dissolution process is increased. An Arrhenius-type plot shown in the Figure 5 (B) gives the relationship of ln I_{peak} and T^{-1} with the equation (7).

$$\ln I_{\text{peak}} = \ln I_0 - \frac{E_A}{RT} \qquad (7)$$

where I_{peak} is the peak current and I_0 is the current at negligible activation barrier. An approximate activation energy (E_A) of 14 kJ mol^{-1} can be calculated from the gradient ($-E_A/R$) of the plot [119,120].

Anthraquinone particles were also immobilised at a basal plane pyrolytic graphite electrode and immersed in aqueous 0.1 M NaOH. In contrast to the temperature-dependent characteristics observed for the reduction of solid immobilised indigo, microparticles of anthraquinone show a reversible reduction response at ca. -0.85 V *vs*. SCE without significant temperature effect. The process is consistent with the two-electron reduction of anthraquinone [121]. The anthraquinol product appears to be sufficiently water insoluble to remain at the electrode surface. Cyclic voltammetry experiments conducted over a range of scan rates (0.05 to 2.0 V s^{-1}, not shown) reveal increased irreversibility at 65 and 75 °C (where loss due to diffusion away from the electrode becomes noticeable) at scan rates of less than 0.1 V s^{-1}. The relatively insignificant temperature effect on the voltammetric response suggests a facile solid state conversion which is approaching completion. The reversible reduction potential for solid anthraquinone appears to be ca. 100 mV negative of that for solid indigo (in aqueous 0.1 M NaOH) and therefore anthraquinone should be an effective redox mediator and catalyst for indigo reduction.

5.2. INDIRECT ELECTROCHEMICAL REDUCTION OF INDIGO (I)

1,8-Dihydroxyanthraquinone (DHAQ) was examined as a possible redox mediator for the indirect electrochemical reduction of indigo. The formal potential for the mediator reduction in 0.1 M phosphate buffer (pH 12, 353 K) $E^{0'} = -0.78$ V *vs*. SCE was noticed to be virtually identical to the reversible potential for the direct reduction of solid indigo ($E^{0'} = -0.78$ V *vs*. SCE) in same medium and therefore it was considered suitable mediator. The schematic picture of the indirect electrochemical reduction of dispersed indigo is shown in the Scheme 4.

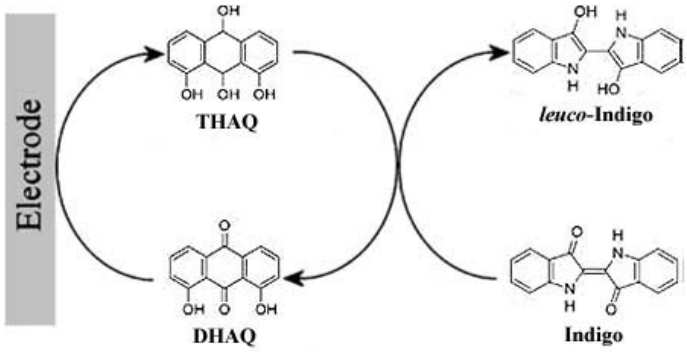

Scheme 4. Diagrammatic representation of the 1,8-dihydroxyanthraquinone mediated reduction of indigo to *leuco*-indigo.

The redox-properties of the DHAQ were identified from the rotating disc measurements which showed the limiting currents of the reversible reduction of the DHAQ. The typical cyclic voltammogram for the DHAQ is shown in the Figure 6**.**

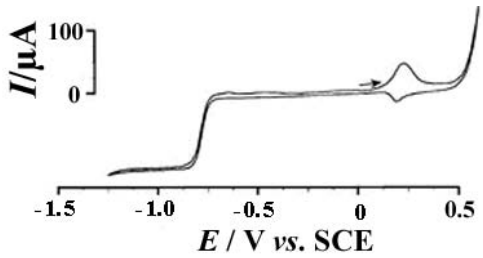

Figure 6. Cyclic voltammogram (scan rate 10 mV s^{-1}) for the reduction of 0.42 mM DHAQ in 0.1 M phosphate buffer pH 12 at a 7-mm-diameter rotating gold disc electrode (5 Hz rate of rotation) at 80 °C with starting potential of 0 V.

The Tomeš criterion [122], which is defined as the potential gap between the points where the current reaches three fourths and one fourth of the limiting current,

$$E_{3/4} - E_{1/4} = 0.035\,V = 2.197 \times \frac{RT}{nF} \qquad (8)$$

(where n is the number of electrons transferred per molecule diffusing to the electrode surface), allows the number of electrons transferred in this electrochemically reversible reduction process to be confirmed as $n \approx 2$ consistent with the proposed mediator reaction in Scheme 4. The oxidation peak at 0.2 V *vs*. SCE is consistent with a gold surface oxidation and not important in this study.

The diffusion coefficient for DHAQ at 80 °C was determined with the Levich equation. The plot of the limiting current observed during reduction *vs*. the square root of the rate of rotation is linear (Figure 7), and therefore, the Levich equation [123] can be employed to determine the diffusion coefficient as shown in the equation (9):

$$I_{lim} = 0.62 \times nFAcD^{2/3}\upsilon^{-1/6}\omega^{1/2} \qquad (9)$$

In this equation the mass-transport-controlled limiting current for the reduction, I_{lim}, is related to the number of electrons transferred per molecule diffusing to the electrode surface, n, the Faraday constant, F, the electrode area, A, the bulk concentration of DHAQ, c, the diffusion coefficient, D, the kinematic viscosity, υ at 80 °C, 0.35×10^{-6} m^2 s^{-1}, and ω, the rate of rotation.

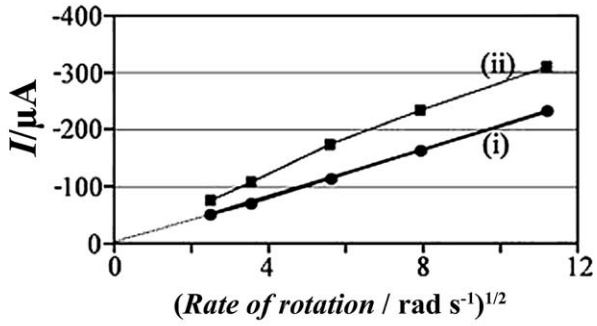

Figure 7. Plot of the limiting currents for the reduction of DHAQ *vs*. square root of the rate of rotation for a solution of 0.42 mM DHAQ (i) without and (ii) with 2 mM colloidal indigo

From data in Figure 7 the diffusion coefficient in 0.1 M phosphate buffer (pH 12) and at a temperature of 80 °C can be determined to be $D = (0.84\pm0.08)\times10^{-9}$ m^2 s^{-1}. Consistent with equation (9) the current was observed to scale linearly with the concentration of the mediator DHAQ. Alkaline solutions of DHAQ were observed to undergo ageing over several days, and therefore, fresh solutions had to be used for experiments.

In the presence of only indigo in alkaline buffer solution, no significant electrochemical reduction current was observed in the absence of the redox mediator even at elevated temperatures of 80 °C. This is consistent with a repulsive or inhibited

interaction between dispersed indigo particles and the electrode surface, also the dispersion of indigo particles through the diffusion is very slow which also accounts to the absence of the direct electrochemical reduction of indigo. However, the current response observed for the redox mediator is substantially increased by the presence of indigo, which is consistent with a mediated reduction of indigo particles (see Figure 7). From the plots of the limiting current *vs*. the square root of rotation rate, it can be seen that the current due to the indigo reduction is characteristically dependent on the rate of electrode rotation.

5.2.1. Analysis of the voltammetric data with simulation (I)

To achieve a more quantitative parameterisation and understanding of the mediated indigo reduction process, a commercial software package for the simulation of voltammetric data, Digisim [113], was employed. Only the limiting currents for the reduction process were considered and simulated. The minimisation of the complexity of the model is important and therefore, the following assumptions were introduced. The dispersed indigo was initially considered to be homogeneously distributed and treated as a molecular species. However, the diffusion coefficient for the indigo species was set to an extremely low limit (here, 10^{-19} m^2 s^{-1}) in order to reflect the low/insignificant mobility of dispersed particles. The mobility of the dispersed particle is considered therefore to be entirely based on convective transport. The mechanism for the mediated indigo reduction is proposed to follow the oversimplified (protonation equilibria are assumed to be fast and ignored) reaction sequence:

$$DHAQ + e^- \rightleftarrows DHAQ^- \quad (10)$$

$$DHAQ^- + e^- \rightleftarrows DHAQ^{2-} \quad (11)$$

$$DHAQ^{2-} + \text{Indigo} \rightleftarrows DHAQ + \textit{leuco}\text{-Indigo} \quad (12)$$

In order to further simplify the analysis, electron transfer in equations (10) and (11) is assumed to be fast (reversible), the equilibrium constant for the process in equation (12) is fixed, K_{eq} = 100, and the forward rate constant, k_{app}, for equation (12) is introduced.

The current responses for DHAQ obtained in the absence of indigo were considered first. Figure 7 shows the characteristic linear Levich behaviour of the current in relation to the square root of the rate of electrode rotation and this behaviour was reproduced with the numerical simulation. The diffusion coefficient, $D = 0.8 \times 10^{-9}$ m^2 s^{-1} at 353 K, was employed for the 1,8-dihydroxyanthraquinone mediator and the simulated currents confirmed the above analysis. The effect of indigo was considered next. Indigo particles are distributed within the solution phase and transport of these particles into the diffusion or reaction layer is assumed to be entirely convection based. A characteristic increase in current was observed experimentally with the indigo addition and it was investigated with the simulation

An overall good match of numerical and experimental data was observed when the forward rate constant for the bimolecular reaction (see equation (12)) was allowed to control the limiting current. In the absence of indigo or for very low chemical rate constants k_{app}, a mediator-only current of -109 μA is determined. For a very high bimolecular rate constant, $k_{app} = 3 \times 10^4$ mol m^{-3} s^{-1}, the expected diffusion-limited current was simulated and it was higher than the experimental current. The diffusion controlled current is not proportional to the concentration of indigo due to the second order nature of the process.

In order to match experimental and simulation currents the value of the apparent bimolecular rate constant was reduced. The best agreement between simulation and experimental data was obtained for an intermediate value of the apparent bimolecular rate constant, $k_{app} = 3$ mol m^{-3} s^{-1}. A remaining trend towards higher simulation currents (compared to experimental currents) at lower rates of electrode rotation can be attributed to the depletion of smaller indigo particles which leads to a change in the apparent rate constant towards smaller values. However, overall the match between experimental and simulation data is good even at different mediator concentrations.

Finally, the effect of the equilibrium constant ($K_{eq} = 100$) for the process given in equation (12) on the kinetic analysis is considered. The reversible potential for both the reduction of indigo and the reduction of the mediator 1,8-dihydroxyanthraquinone at

80 °C are virtually identical and therefore the (simplifying) choice of a very large equilibrium constant could be criticized. However, voltammetric data simulated for the process described by equations (10), (11) and (12) is rather insensitive to the magnitude of this equilibrium constant and even when set to unity very similar currents are simulated. Therefore the apparent bimolecular rate constant determined in this approach can be considered reliable.

5.2.2. Interpretation of the rate constant (I)

Indigo particles create their own diffusion field and the rate of diffusion of the redox mediator towards the particle has to be considered. The apparent bimolecular rate constant determined experimentally has to be written as in equation (13).

$$\frac{\mathrm{d}[\mathit{leuco}-\mathrm{indigo}]}{\mathrm{d}t} = k_{\mathrm{app}} \times [\mathrm{indigo}] \times [\mathrm{mediator}] \qquad (13)$$

In this equation the concentration term [indigo] is introduced to denote not molecularly dispersed indigo but a particulate species and the apparent bimolecular process is interpreted as a surface reaction. The rate of formation of *leuco*-indigo is related to an apparent rate constant k_{app}, the concentration of indigo and the concentration of the reduced form of the redox mediator. For the case of diffusion control this equation may also be written as in equation (14) [120].

$$\frac{\mathrm{d}[\mathit{leuco}-\mathrm{indigo}]}{\mathrm{d}t} = 4\pi\, rD \frac{N_{\mathrm{A}}}{N_{\mathrm{P}}} \times [\mathrm{indigo}] \times [\mathrm{mediator}] \qquad (14)$$

In this equation the diffusion controlled rate of formation of *leuco*-indigo is related to D, the diffusion coefficient for the redox mediator, N_{A} , Avogadro's number, and N_{P} , the number of indigo molecules per particle and particle radius, r. The parameters r (the particle radius) and N_{P} (the number of indigo molecules per particle) are related (by $\frac{N_{\mathrm{P}}}{N_{\mathrm{A}}} \times \frac{M}{\rho} = 4\pi\, r^3$, with the molecular mass M and the density ρ) and with k_{app} known they can be determined employing equations (15) and (16).

$$r = \sqrt{\frac{DM}{k_{\text{app}}\rho}} \tag{15}$$

$$N_{\text{P}} = 4\pi N_{\text{A}} \sqrt{\frac{M}{\rho}\left(\frac{D}{k_{\text{app}}}\right)^3} \tag{16}$$

With parameters determined in this study (k_{app} = 3 mol m^{-3} s^{-1} , D = 0.84× 10^{-9} m^2 s^{-1} , M = 262 g mol^{-1}, and ρ is assumed 10^6 g m^{-3}) the approximate particle radius r = 0.27 μm and N_{P} = 6 × 10^8 molecules were estimated. A consistent mechanistic picture of the mediator-based reduction of indigo was obtained based on a diffusion controlled reductive dissolution of dispersed indigo particles.

5.3. GLUCOSE-ASSISTED REDUCTION OF INDIGO (II,III,IV)

The dissolution of indigo in aqueous media is a heterogeneous process which is likely to involve a surface confined reaction step. The surface area of the particulate and highly water insoluble indigo is therefore controlling the rate of dissolution. Dissolution reactions have been treated in the literature for example for spherical [124] or for cylindrical particles [125].

Here, indigo particles were assumed to be spherical (Scheme 5) and uniformly sized (for simplicity) and the rate law for the reductive dissolution of indigo to *leuco*-indigo in the presence of excess glucose is given by equation (17).

$$\frac{\mathrm{d}n_{leuco-\text{indigo}}}{\mathrm{d}t} = k' \times S_{\text{indigo}} \tag{17}$$

In this equation $n_{leuco\text{-indigo}}$ is the molar amount of *leuco*-indigo produced, *k'* is a chemical dissolution rate constant (in mol s^{-1} m^{-2}) and the surface area $S_{\text{indigo}} = 4\pi r^2$ (with r the approximate radius of the indigo particles).

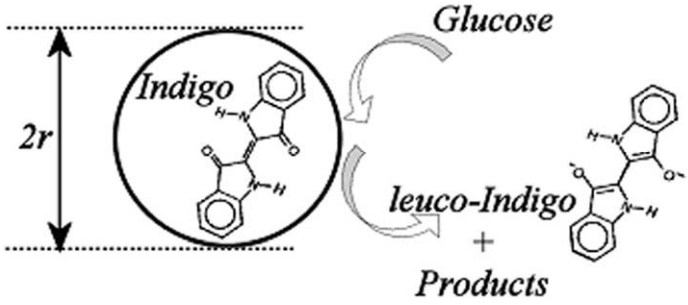

Scheme 5. The glucose driven reduction of indigo.

If a spherical indigo particle is assumed, the amount of indigo, n_{indigo}, in the suspension is determined by the radius r, the density ρ, and the molar mass M (equation (18)).

$$n_{\text{indigo}} = \frac{\rho}{M}\frac{4}{3}\pi r^3 \tag{18}$$

The rate of reductive indigo dissolution is then equivalent to the rate of *leuco*-indigo formation and given by the change in particle radius (Equation (19)).

$$\frac{\mathrm{d}n_{\text{leuco-indigo}}}{\mathrm{d}t} = -\frac{\rho}{M}4\pi r^2\frac{\mathrm{d}r}{\mathrm{d}t} \tag{19}$$

Comparison of equations (17) and (19) suggests an expression for the change in particle radius with time.

$$k' \times S_{\text{indigo}} = -\frac{\rho}{M}4\pi r^2\frac{\mathrm{d}r}{\mathrm{d}t} \tag{20}$$

$$\frac{\mathrm{d}r}{\mathrm{d}t} = -k' \times \frac{M}{\rho} \tag{21}$$

$$r(t) = r_0 - k' \times \frac{M}{\rho} \times t \tag{22}$$

The concentration of *leuco*-indigo as a function of time is then obtained by combining equations (18) and (22) (equation (23)).

$$n_{leuco-\text{indigo}}(r_0,t) = n_{\text{indigo}}(r_0,0) - n_{\text{indigo}}(r_0,t) = n_{\text{indigo}}(r_0,0) - \frac{\rho}{M}\frac{4}{3}\pi\left(r_0 - k' \times \frac{M}{\rho} \times t\right)^3 \quad (23)$$

The initial rate of *leuco*-indigo formation can be obtained by derivation (equation (24)).

$$\left(\frac{\mathrm{d}n_{leuco-\text{indigo}}}{\mathrm{d}t}\right)_{t=0} = k' \times 4\pi r_0^2 \quad (24)$$

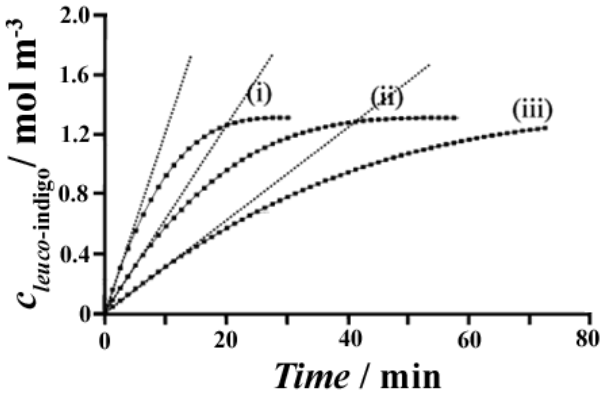

Figure 8. Predicted plots of the concentration of *leuco*-indigo formed during reductive dissolution of indigo. Parameters are r_0 = 0.5 μm, M = 0.262 kg mol^{-1}, ρ = 1451 kg m^{-3}, and a rate constant of (i) k'= 7.7 × 10^{-6} m s^{-1} × 200 mol m^{-3}, (ii) k'= 4.1 × 10^{-6} m s^{-1} × 200 mol m^{-3}, (iii) k'= 2.0 × 10^{-6} m s^{-1} × 200 mol m^{-3}. The dashed line indicates the initial rate.

Equation (23) allows the change in *leuco*-indigo concentration with time to be plotted. Figure 8 shows plots of the concentration of *leuco*-indigo generated for an amount of indigo particles equivalent to a 1.3 mM concentration with an assumed radius of r_0 = 0.5 μm. The molar mass M = 0.262 kg mol^{-1}, and the density ρ = 1451 kg m^{-3} [48,126] were used. The predicted time dependence is consistent with the experimentally observed curves and both the initial rate and the end point plateau data are readily obtained. The initial rate (see dashed line) is the most convenient way of extracting the rate constant for indigo dissolution. The more linear shape in experimental data plots is caused by the effect of the particle shape.

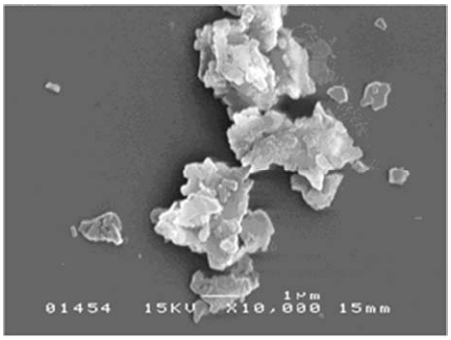

Figure 9. Scanning electron micrograph for typical indigo crystals.

Figure 9 shows an SEM image of typical indigo particles. These particles crystallise in small platelets. The (during crystallisation) rapidly growing edges of the platelets are likely to be more reactive also during reductive dissolution and therefore the "active" surface area will be dominated by these edge areas rather than the plane area. Directed hydrogen bonding within the solid state structure is responsible for this effect [127]. This geometric anisotropy will dominate the rate of dissolution which then remains almost constant over the whole course of reaction. This results in an almost constant reaction rate (see equation (17)) and therefore in a much more linear increase in *leuco*-indigo concentration (in contrast to the more curved plots predicted based on the approximate sphere model). However, the use of the initial rate data (as employed here) will produce reliable rate constant data in both cases.

5.3.1. Rotating disc voltammetry (II)

The electrochemical response for glucose at a glassy carbon electrode immersed in alkaline solution was investigated first without indigo addition. Figure 10 shows the oxidation response for a solution of 22 mM D-(+)-glucose in 0.2 M NaOH (65 °C) developing with time. A clear but broad oxidation response is observed at ca. -0.1 V *vs*. SCE (Process 1). Initially this process is absent but with time this response gradually increases indicating a chemical reaction which leads to the formation of a readily oxidisable intermediate from glucose and this intermediate is most likely active in the reduction of indigo. The alkaline degradation process of glucose is complex and the degradation products, specifically the active intermediate, haven't been identified in the conditions used in these experiments.

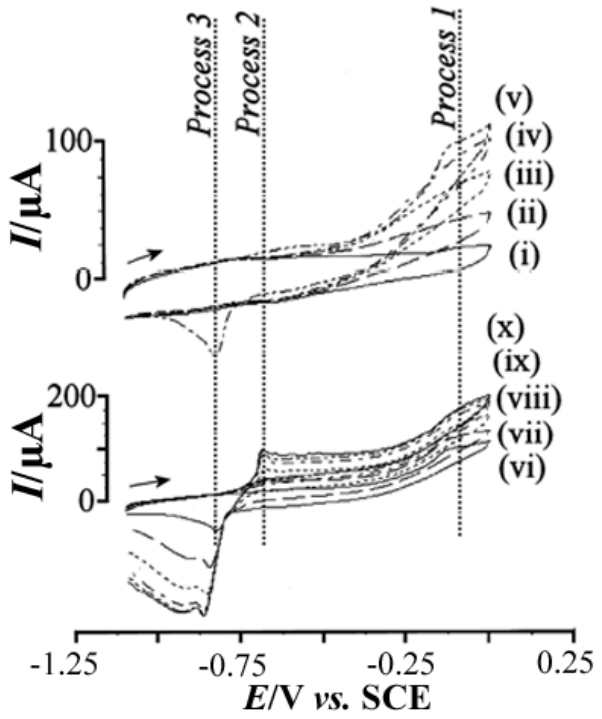

Figure 10. Cyclic voltammograms (scan rate 10 mV s^{-1}, rotation rate 5 Hz) for D-(+)-glucose (22 mM) in aqueous 0.2 M NaOH at 65 ^{o}C obtained at a rotating 3 mm diameter glassy carbon disc electrode with starting potential -1.1 V. The current was monitored for (i) 0 min, (ii) 5 min, (iii) 10 min, (iv) 15 min after glucose addition. Next, indigo (1.33 mM) was added 20 minutes into the experiment and further cyclic voltammograms are recorded at (v) 20 min, (vi) 25 min, (vii) 30 min, (viii) 35 min, (ix) 40 min, and (x) 45 min.

After a delay of 20 minutes, indigo (equivalent to 1.33 mM) was added into the reaction mixture. No direct reduction of indigo at the glassy carbon electrode surface was observed. Therefore, *leuco*-indigo formed due to chemical reduction of indigo can be observed very clearly. Immediately after indigo addition (see Figure 10 (v)) a small anodic current (Process 2) and a new cathodic peak current (Process 3) are observed.

Processes 2 and 3 are consistent with the oxidation and re-reduction of *leuco*-indigo in solution (equation (25)) with a midpoint potential of -0.75 V *vs*. SCE. This onset of the indigo reduction process occurs at a considerably more negative potential when compared to the oxidation of glucose intermediate and therefore the reduction of indigo by glucose may be expected to be kinetically very slow. The peak for the cathodic

process (Process 3) is associated with the "stripping" of a small amount of solid indigo from the electrode surface back into solution.

Process 2 *leuco*-indigo (aq) → indigo (solid) + 2 e^- (25a)

Process 3 indigo (solid) + 2 e^- → *leuco*-indigo (aq) (25b)

Voltammetric currents observed under rotating disc conditions are governed by convection processes [119], and the mass transport controlled limiting current is directly proportional to the concentration of the reacting species in the bulk solution [123]. That is, for Process 2 the observed limiting current is directly proportional to the concentration of *leuco*-indigo. When the plots of the limiting currents *vs*. time were drawn approximately linear change in *leuco*-indigo concentration was observed. This was true also when indigo was added at the same time as glucose. The slopes were also similar in both occassions (the results not shown). The similarity of these slopes suggested that the formation of *leuco*-indigo is kinetically limited and the formation of the electroactive reductant derived from glucose is not crucial or rate determining under these conditions. A slow heterogeneous chemical step represented by the heterogeneous dissolution rate constant is likely.

The progress of the formation of *leuco*-indigo in the presence of glucose can clearly be followed by observing the mass transport controlled limiting current for the oxidation of *leuco*-indigo (Process 2). By varying the ratio of glucose to indigo further information about the stoichiometry of the process is obtained. Figure 11 shows plots of limiting current data when indigo was added at the same time as glucose was. Doubling the glucose concentration has no significant effect on the rate of *leuco*-indigo formation while reducing the concentration of indigo from 5.7 to 2.9 to 1.3 mM (based on moles insoluble solid per volume solution) clearly reduces the final amount of *leuco*-indigo produced.

The rate of *leuco*-indigo formation is approximately the same when the glucose concentration is altered but it appears to be proportional to the amount of indigo present (or the surface area of indigo particles in suspension, see equation (17)). In all

cases the time required for full conversion remains approximately the same. The final stage of the reaction where a current plateau is observed is consistent with the recoloration of the reaction mixture (the dark blue colour changes into yellow-brown) and with the complete conversion of indigo to *leuco*-indigo. Exposure of the resulting solution to air immediately caused the formation of dark blue indigo from the dissolved *leuco*-indigo.

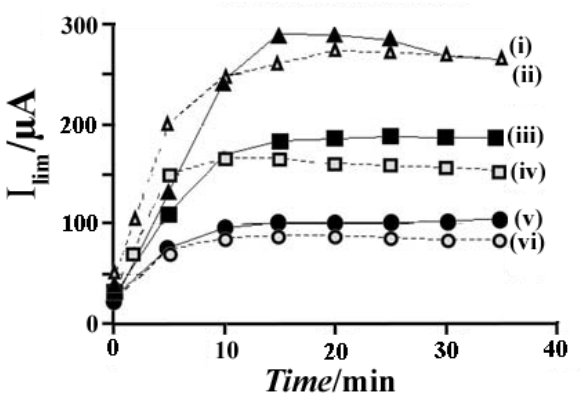

Figure 11. The effect of glucose and indigo concentrations on the rate of *leuco*-indigo formation in 0.5 M NaOH: (i) 22 mM glucose, 5.7 mM indigo; (ii) 44 mM glucose, 5.7 mM indigo; (iii) 22 mM glucose, 2.9 mM indigo; (iv) 44 mM glucose, 2.9 mM indigo; (v) 22 mM glucose, 1.3 mM indigo; (vi) 44 mM glucose, 1.3 mM indigo.

When the NaOH concentration was increased from 0.1 to 0.5 M both the rate and extent of *leuco*-indigo reduction increased (Figure 12), and the rate equation given in equation (17) may be modified to give the following rate law :

$$\frac{\mathrm{d}n_{leuco-\mathrm{indigo}}}{\mathrm{d}t} = k' \times S_{\mathrm{indigo}} = k \times c_{\mathrm{OH^-}} \times S_{\mathrm{indigo}} \qquad (26)$$

The rate expression (equation (26)) allows the individual rate constants *k'* to be determined as a function of hydroxide concentration and this allows k = 4.1 (±0.3) × 10^{-9} m s^{-1} (at 65 °C) to be estimated. An additional effect observed in the presence of different NaOH concentrations is the change in the final limiting current. At lower hydroxide concentration clearly the final current plateau is reduced. However, it is very likely that this effect is introduced due to the diffusion coefficient of the resulting

leuco-indigo in the aqueous electrolyte. A higher alkalinity may be better for preventing aggregation effects and for generally improving *leuco*-indigo solubility and diffusivity. At 0.1 M NaOH there was also evidence of incomplete conversion of indigo and therefore lower final *leuco*-indigo concentration in the solution.

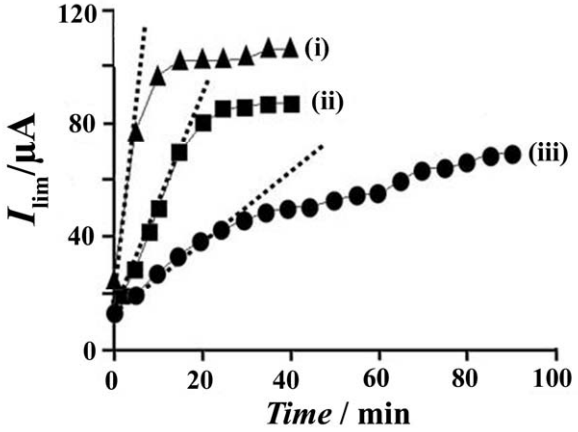

Figure 12. The effect of the NaOH concentration on the rate of leuco-indigo formation: (i) 1.3 mM indigo, 22 mM glucose, 0.5 M NaOH; (ii) 1.3 mM indigo, 22 mM glucose, 0.2 M NaOH; (iii) 1.3 mM indigo, 22 mM glucose, 0.1 M NaOH.

Hydrodynamic cyclic voltammograms were measured at three different temperatures; 55, 65 and 75 ºC, and there was clear evidence of the temperature strongly affecting the rate of indigo reduction, so that higher the temperature faster the reaction. Activation energy was estimated to be 64 kJ mol^{-1} from the Arrhenius plot (not shown).

5.3.2. Sonoelectrochemistry (II,III,IV)

Sonovoltammetry was employed as one of the options of studying hydrodynamically the glucose-assisted reduction of indigo. Strong agitation was produced by a power ultrasound (24 kHz) horn system where the horn was positioned opposite to the working electrode (see Figure 3.) [128]. In addition to the agitation the power ultrasound applied to electrodes can lead to surface cleaning effects and higher reproducibility [129,130]. The final limiting current after complete reductive dissolution of indigo was increased when the horn to electrode distance was decreased due to more intense agitation close to the horn system. The rate parameters obtained in

these measurements were virtually identical to those obtained with the rotating disc methods.

Another method of sonovoltammetry was introduced where the electrode was the source of vibration and no external agitation was necessary. The use of hydrodynamic electrode system allows diffusion controlled signals to be enhanced and in particular vibrating electrodes [131,132] provide a high rate of mass transport and simple operation. Vibrating probe systems are simple devices with no special requirements in terms of cell geometry or sample pretreatment and without complex moving parts. Vibrating electrode systems have been employed previously in electroanalysis as hydrodynamic sensor [133] and for heavy metal stripping analysis [134].

A 250 Hz laterally vibrating electrode was developed for the *leuco*-indigo measurement (see Figure 4). In order for this sonoprobe system to be employed the mass transport effects at the electrode surface had to be understood and calibrated. So the mass transport conditions at the vibrating electrode surface were characterised with the known $Fe(CN)_6^{3-/4-}$ redox system. The peak or limiting currents for the oxidation of ferrocyanide to ferricyanide were measured at different scan rates for different vibrational amplitudes (no vibration, low and high vibrational amplitude) and for different temperatures. The diffusion coefficients for ferrocyanide were calculated based on the appropriate Randles-Sevcik equation [135] where the peak currents for the non-vibrational voltammograms were a function of scan rates (v) (see equation (27)).

$$I_{\text{peak}} = 0.4463nFAc\sqrt{\frac{nFDv}{RT}} \qquad (27)$$

In this equation n is a number of electrons transferred per molecule diffusing through to the electrode surface. Analysis of the data with the equation (27) suggested approximate diffusion coefficients for ferrocyanide to be at different temperatures: $D_{55}=1.3\times10^{-9}$ m^2 s^{-1}, $D_{65}=1.5\times10^{-9}$ m^2 s^{-1}, $D_{75}=1.7\times10^{-9}$ m^2 s^{-1} which are in good

agreement with the literature [136]. The diffusion layer thickness (δ) values were determined with the Nernst diffusion layer model [137,138].

$$I_{\lim} = \frac{nFDAc}{\delta} \qquad (28)$$

Diffusion layer thicknesses were estimated to be approximately 5.0 μm and 7.0 μm at low and high vibrational amplitudes respectively.

Figure 13 (A) shows a typical set of voltammograms obtained for the oxidation of 1.1 mM *leuco*-indigo in 0.2 M NaOH at 75 °C at a vibrating (low amplitude) 500 μm diameter gold electrode. The reduction of indigo to *leuco*-indigo was performed in situ with glucose and this had the advantage over dithionite as reductant in that glucose does not cause any interfering electrode process. Figure 13 (B) shows a typical set of voltammograms obtained under similar conditions and for three different concentrations of *leuco*-indigo. Based on these data, Process 1 at a potential of -0.6 V *vs*. SCE is consistent with the mass transport controlled limiting current for the oxidation of *leuco*-indigo. At more positive potentials a broad response is observed (Process 2) which is linked to the oxidation of glucose. Due to the formation of insoluble indigo at the electrode surface, blocking occurs with time and both the *leuco*-indigo oxidation (Process 1) as well as the glucose oxidation (Process 2) are affected.

Figure 13 (A) clearly demonstrates the effect of indigo blocking the electrode to increase as the scan rate decreases. After reversal of the scan direction a further peak response (cathodic) is observed at a potential of -0.9 V *vs*. SCE (see Process 3) consistent with the electrochemical ‘‘stripping’’ response of solid indigo adhering to the gold electrode surface. It can be concluded that in order to improve the analytical signal (Process 1) (i) the scan rate has to be high (up to 4 V s^{-1}), (ii) the vibrational amplitude is preferred to be low (faster mass transport also leads to faster blocking), and (iii) the temperature has to be high.

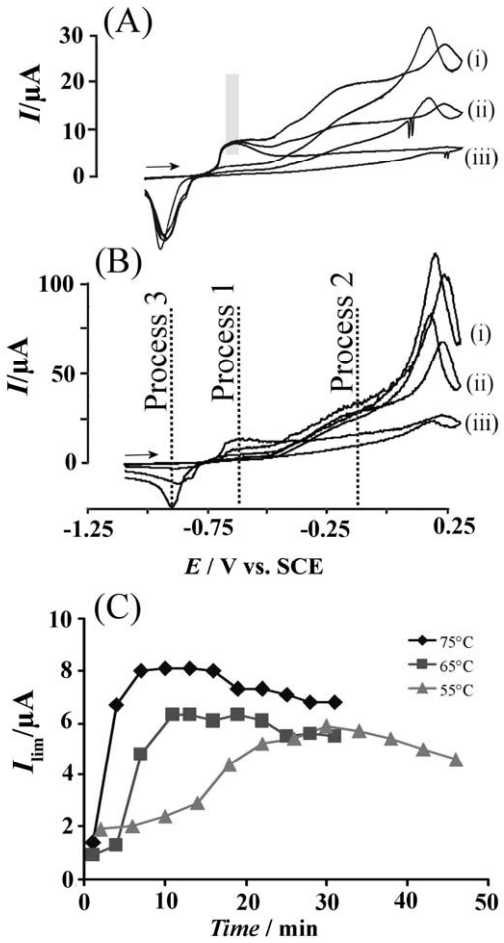

Figure 13. Cyclic voltammograms (scan rate (i) 90, (ii) 60, and (iii) 50 mV s^{-1}) for the oxidation and re-reduction of 1.1 mM *leuco*-indigo (dissolved in 33 mM glucose in 0.2 M NaOH at 75 ºC) at a vibrating (low amplitude) 500 µm diameter gold disc electrode with starting potential of -1.1 V. The grey zone indicates the steady state limiting current region. (B) Cyclic voltammograms (scan rate 200 mV s^{-1}) for the oxidation and re-reduction of (i) 0.34 mM, (ii) 1.1 mM, and (iii) 1.8 mM *leuco*-indigo in 0.2 M NaOH at 75 ºC at a vibrating (low amplitude) 500 µm diameter gold disc electrode. (C) Plot of the limiting current versus time showing the formation of the *leuco*-indigo for 1.1 mM indigo (suspended in 33 mM glucose in 0.2 M NaOH) at temperatures of 55, 65, and 75 ºC at potential -0.6 V *vs*. SCE.

With the voltammetric technique, the chemical indigo reduction process (with glucose in 0.2 M NaOH) was monitored by measuring the mass transport controlled limiting current (Process 1) for the oxidation of *leuco*-indigo every 3 min. Figure 13 (C) shows the time dependence of the *leuco*-indigo concentration at three different temperatures:

55, 65, and 75 °C. The plateau reached at the highest limiting current shows that the reaction has gone to completion (simultaneously a colour change from dark blue to yellow-brown occurred). The slow decrease of the plateau current at longer times (more than 15 min after the plateau is reached) can be attributed to a slow loss of the reducing power after glucose decomposition and possibly also to traces of oxygen leaking into the cell, it is also possible that the electrode is blocked more and the "stripping" no longer helps. From the temperature effect on the slope of *leuco*-indigo formation *vs*. time, it can be seen that the rate of indigo reduction is approximately doubled for each 10 °C increase in temperature (the approximate activation energy for the heterogeneous reduction of indigo is 65 kJ mol^{-1}).

It would be possible to perform the indigo determination even faster at even higher temperatures, but the temperature effect on the seal in the PEEK mounting of the vibrating electrode prevented work at temperatures higher than ca. 75 °C. Also the increase in the final limiting current (see Figure 13 (C)) is consistent with the faster rate of diffusion of the *leuco*-indigo molecules in a less viscous solution (at higher temperature). The diffusion coefficients for *leuco*-indigo can be estimated from the limiting currents (Process 1) based on the $Fe(CN)_6^{3-/4-}$ calibration data and equation (28). Assuming a two-electron oxidation, the estimated diffusion coefficients for *leuco*-indigo are: $D_{55}=0.9\times10^{-9}$ m^2 s^{-1}, $D_{65}=1.1\times10^{-9}$ m^2 s^{-1}, $D_{75}=1.3\times10^{-9}$ m^2 s^{-1}. These values are in good agreement with estimates for these diffusion coefficients based on the Wilke–Chang expression [139].

As already determined with the rotating disc electrode the NaOH concentration affects the rate of *leuco*-indigo formation. Figure 14 shows the plots of limiting currents of the oxidation of *leuco*-indigo at different NaOH concentrations. The colour of the suspension in 0.1 M NaOH remains dark, consistent with incomplete conversion of indigo whereas in 0.2 M NaOH the colour changes. Therefore, the concentration of NaOH is a crucial parameter in the effectiveness of the overall reduction process. It is possible that the ability of glucose to generate a powerful reducing agent depends on the level of hydroxide present in solution.

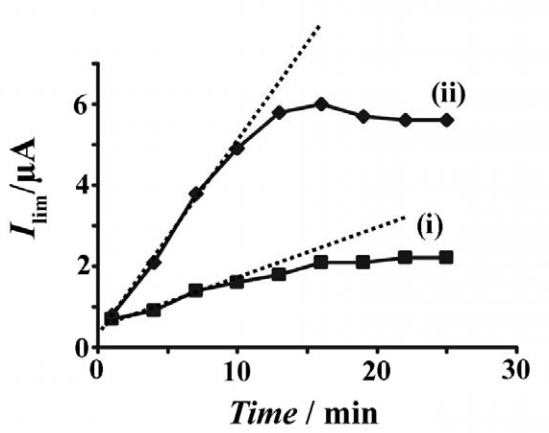

Figure 14. Plot of the limiting currents at potential -0.6 V *vs*. SCE of the *leuco*-indigo oxidation versus time at (i) 0.1 M and (ii) 0.2 M NaOH when 1.1 mM indigo is reduced with 22 mM glucose at 65 °C.

Furthermore, the lack of progress in the reductive dissolution in low NaOH concentrations is also linked to the activity of Na^+ which is competing with protons for the anionic binding sites on the surface of the reacting indigo crystal. In order to improve the rate and efficiency of the indigo reduction (while limiting the need for alkali during the process), redox catalysts can be introduced. Anthraquinone as well as its derivative 1,8-dihydroxyanthraquinone (DHAQ) can be used as catalysts for the glucose assisted reduction of indigo.

5.4. ANTHRAQUINONE CATALYSED REDUCTION OF INDIGO WITH GLUCOSE (II,III,IV)

Both the relatively small magnitude of the dissolution rate constant and the high activation energy suggest that a slow chemical reaction step governs the reductive dissolution of indigo. Anthraquinone derivatives are known to act as electron transfer mediators in the electrochemical reduction of indigo [18]. In particular 1,8-dihydroxyanthraquinone is a very effective mediator for this reaction. The DHAQ solution was added in the NaOH solution at the same time with glucose and indigo. Figure 15 shows the effect of the 1,8-dihydroxyanthraquinone mediator on the reduction of indigo by glucose at 0.1 M NaOH measured with the rotating disc electrode. The DHAQ mediator seems to have a strong catalytic effect on the reduction process. The reaction rate is increased even at lower NaOH concentrations.

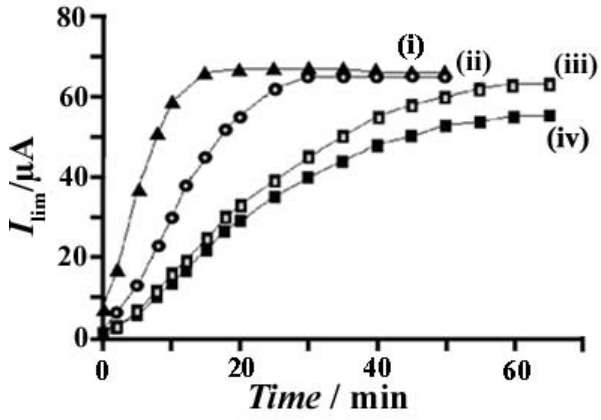

Figure 15. Plots are shown for the limiting currents for *leuco*-indigo (3 mm diameter glassy carbon rotating disc electrode, rotation speed 5.0 Hz) for the reduction of indigo (1.3 mM) by glucose (22 mM) at a temperature of 65 °C with and without different concentrations of DHAQ in 0.1 M NaOH: (i) 320 μM, (ii) 32 μM, (iii) 3.2 μM, and (iv) no DHAQ.

Many anthraquinone derivatives are toxic but the parent anthraquinone is considered relatively safe to use [140] and readily available. The insignificant solubility of anthraquinone in aqueous media can be sidestepped in the present work by direct impregnation of the redox catalyst onto the indigo substrate prior to the reduction experiments. The anthraquinone catalyst was dissolved in acetone, indigo particles suspended into this solution by sonication, and after complete evaporation of the solvent, indigo, on which anthraquinone had been uniformly immobilised, was obtained. The amount of anthraquinone on the indigo surface was altered to determine the lowest effective level of catalyst.

The catalytic effect of anthraquinone on the glucose assisted reduction of indigo was measured with the sonoprobe introduced earlier. Figure 16 (A) shows plots for the formation of *leuco*-indigo from anthraquinone-dosed indigo. In contrast to what happens in the absence of anthraquinone, the reduction process is highly effective in the presence of the lower concentration (0.1 M) of NaOH, and indigo is completely converted to *leuco*-indigo within 10-15 minutes (compare Figure 14). Low levels of anthraquinone effectively increase the rate and conversion level of the reduction process. At a level of 0.3 mol% (corresponding to 3 μM) the catalyst is still fully active and only at 0.1 mol% is the effect lost. In comparison, a solution of 3 μM water-

soluble 1,8-dihydroxyanthraquinone catalyst had virtually no effect, instead 32 μM DHAQ was the lowest concentration where there was still strong catalytic effect to the reduction of indigo (see Figure 15).

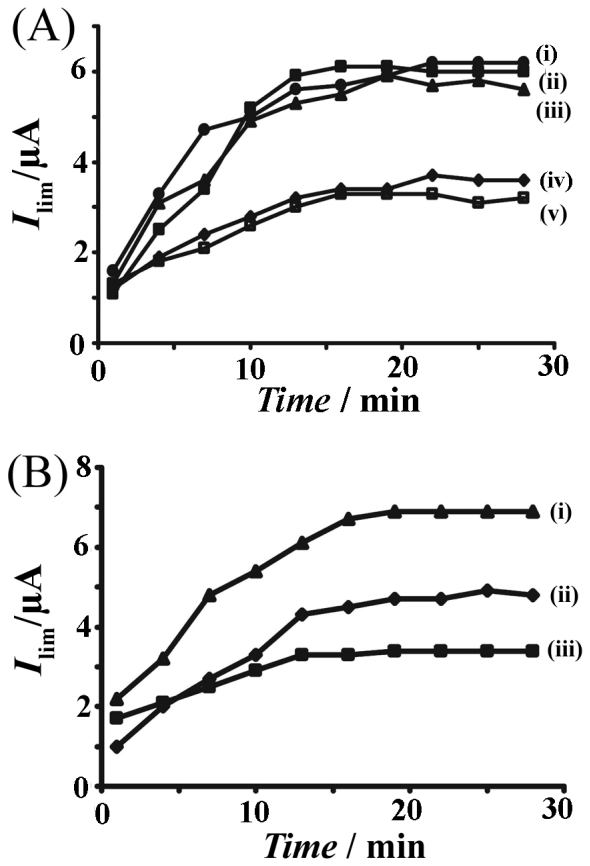

Figure 16. (A) Plots of the limiting currents at potential -0.6 V *vs*. SCE of the *leuco*-indigo oxidation versus time for the reduction of 30 mg of indigo (corresponding to 1.1 mM) with 22 mM glucose in 100 cm^3 aqueous 0.1 M NaOH at 65 °C. The concentration of anthraquinone (present as solid) was (i) 30 μM, (ii) 15 μM, (iii) 3.0 μM, (iv) 1.5 μM, and (v) 0.8 μM. (B) Plots of the limiting currents of the *leuco*-indigo oxidation versus time for the reduction of 30 mg of indigo (corresponding to 1.1 mM) with 22 mM glucose in 100 cm^3 aqueous NaOH at 65 °C in the presence of 15 μM anthraquinone with (i) 0.1 M, (ii) 0.08 M, and (iii) 0.05 M NaOH.

With insufficient amounts of anthraquinone (less than 3 μM) the indigo reduction process fails to go to completion and the suspension remains dark. Increased amounts of catalyst above the critical level do not significantly speed up the reduction process either (see Figure 16 (A)). Excess of anthraquinone catalyst is likely to remain

insoluble and inactive under the reaction conditions employed. These findings suggested that it would be profitable to determine if the NaOH concentration could be lowered even further in the presence of anthraquinone catalyst, but Figure 16 (B) demonstrates that lowering the concentration of NaOH significantly below 0.1 M is not compatible with the full reduction of indigo (at 65 °C). It was noted that the suspension remained dark and therefore the reduction incomplete even after the plateau level of *leuco*-indigo had been reached.

The effect of glucose on the reduction process was followed. Glucose is present typically in 20-fold excess and halving the concentration of glucose appears to not affect significantly the progress of the reaction. Halving the concentration of glucose again, however, does affect the process. An excess of at least 10-fold of glucose versus indigo appears to be necessary for the reaction to go to completion (in the presence of 15 µM anthraquinone and at 65 °C). The rate of *leuco*-indigo formation was followed by voltammetry at temperatures of 55, 65, and 75 °C. Increasing the temperatures significantly accelerates the reduction of indigo and from the approximate rate of *leuco*-indigo formation the Arrhenius activation energy can be estimated to be 120 kJ mol^{-1}. This is relatively high, it is indicative of a high activation barrier, almost twice as high as that observed for the same process in the absence of the anthraquinone catalyst.

5.5. INDIGO SUBLIMATION AND SEM (IV)

Indigo crystals of almost macroscopic size can be grown in short-path sublimation experiments to obtain plate-like crystals that owe their appearance to the layered packing in the indigo crystal structure. Figure 17 shows the indigo structure from three directions (red = O, blue = N, green = C) and the sheet-like structures held by the strong inter-molecular hydrogen bonds are clearly visible.

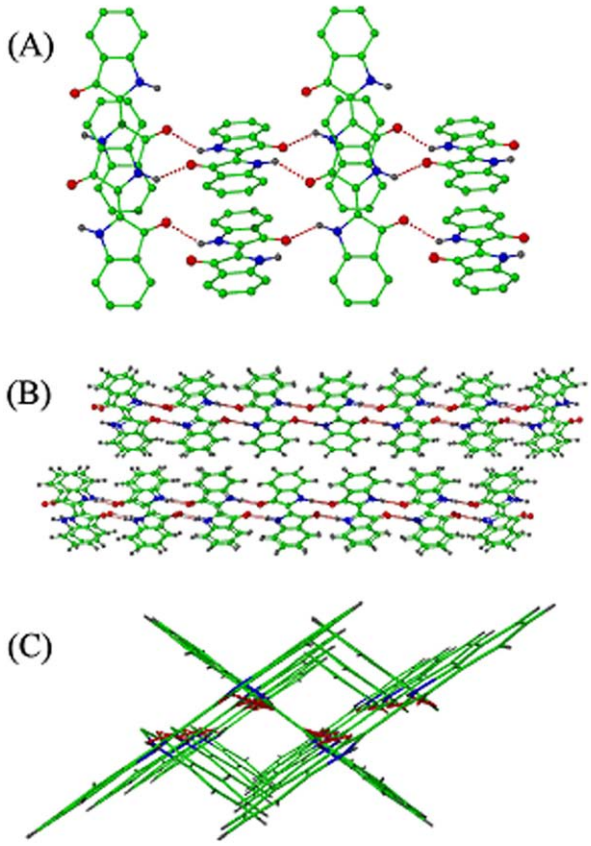

Figure 17. Crystal structure of indigo showing (A) from the top onto an indigo sheet, (B) from the side on two indigo sheets, and (C) from the side into a single indigo sheet. Within sheets, oxygen (red) and nitrogen (blue) atoms are inter-linked via hydrogen bonds (dashed lines).

The sheet structure at molecular level is reflected in the formation of thin crystal plates at macroscopic level. During the indigo reduction process, both, the interactions between sheets and the stronger interactions within sheets need to be overcome. Indigo crystals grown by sublimation were immobilised onto sticky carbon tape (for mounting SEM samples) and imaged by electron microscopy (after gold sputter coating). Figure 18 (A) shows a typical assembly of plate-like crystals with many smaller crystal debris visible initially. The characteristic shape of the crystals originates from the preferred growth direction planar to the sheet. In order to monitor the indigo reduction, samples of immobilised indigo crystals were immersed in glucose-containing reduction solution and withdrawn at various times.

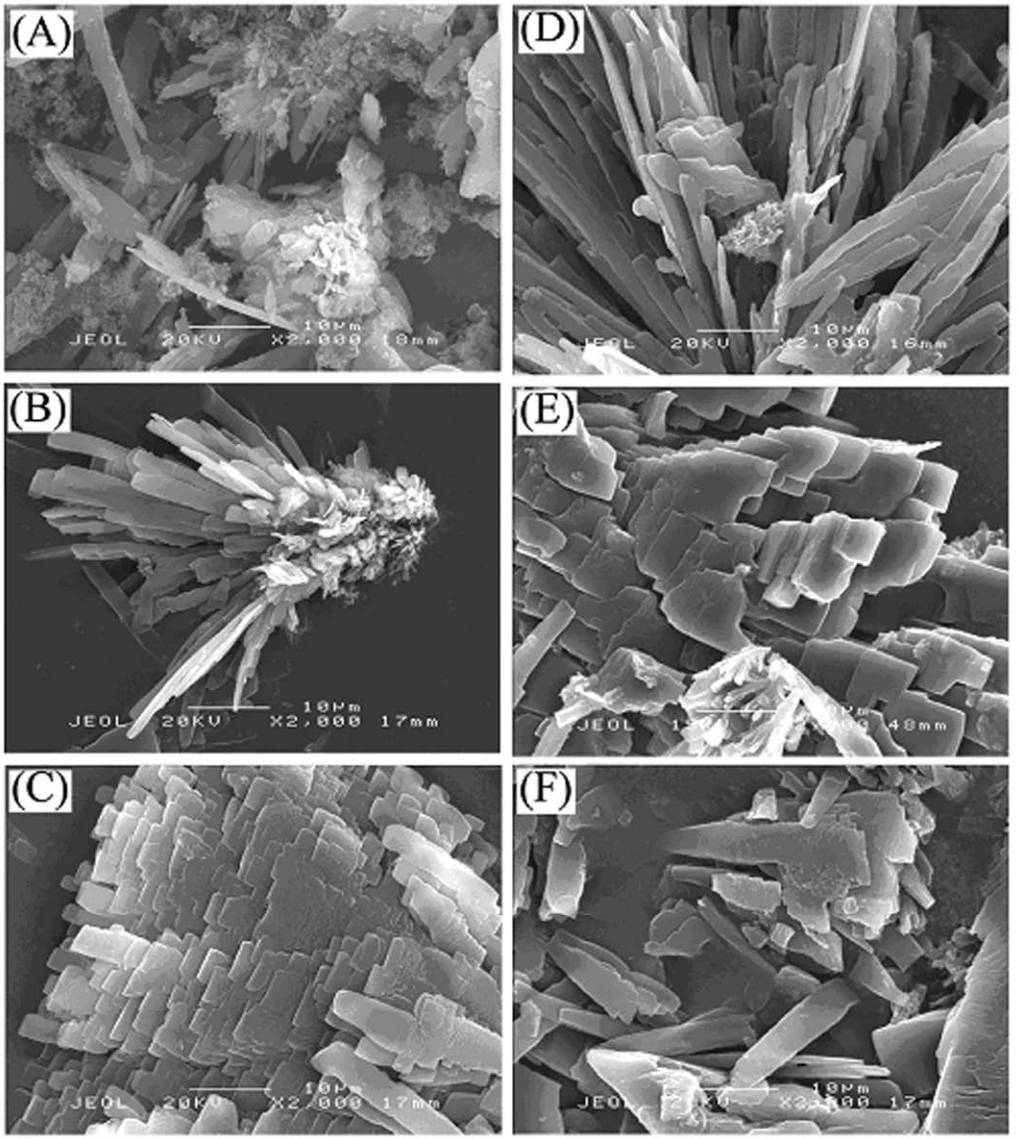

Figure 18. SEM images (low magnification) of indigo crystals (A) before reduction, (B) after 3 minute reduction, (C) after 14 minute reduction, (D) anthraquinone-dosed after 3 minute reduction, (E) anthraquinone-dosed after 15 minute reduction, and (F) anthraquinone-dosed after 25 minute reduction. The reduction was achieved by immersion into aqueous 0.2 M NaOH with 22 mM glucose at 65 °C which was followed by rinsing with water and drying.

Figure 18 (B) and (C) show samples after 3 minutes and after 14 minutes reduction. The smaller indigo crystal debris was immediately removed. Larger crystals remained and were still observed after 14 minutes of reduction. When the experiment was

repeated with anthraquinone-dosed indigo (see Figure 18 (D), (E), and (F)) similar images to those obtained with untreated indigo were obtained. In all cases the plate-shape of indigo crystals remains and no holes are formed. It is most likely that the reductive dissolution process occurs from the edges and that this process is relatively slow perpendicular to the indigo sheets. Closer inspection of Figure 18 (C) and (F) shows etch patterns and terrace-like features which are typical for reductive dissolution occurring from the edges. In the presence of anthraquinone there appear to be more irregular features possibly associated with local anthraquinone concentration variations. Although quantitative information is not obtained from these images, qualitatively they support the idea of a reductive dissolution process occurring at the edges of indigo crystals.

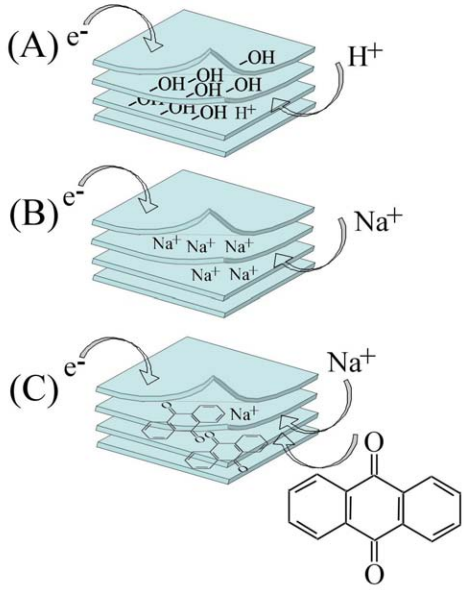

Figure 19. Schematic representation of the indigo reduction process at the edge of a layered indigo crystal with (A) proton intercalation, (B) Na^+ intercalation, and (C) simultaneous anthraquinone and Na^+ intercalation.

Figure 19 shows a schematic representation of three types of reductive dissolution. In the presence of protons the reduction is limited to the edges of indigo sheets and proton intercalation followed by delamination and further dissolution is unlikely to occur. The protons block further progress of the reductive dissolution. In contrast, sodium cations can intercalate, which, under sufficiently alkaline conditions, will lead to slow

delamination and disintegration of the indigo sheets. Finally, in the presence of anthraquinone, strong adsorption of the planar anthraquinone molecule into the gap between indigo sheets occurs and the catalyst is moving into the crystal like a "wedge" causing more rapid delamination and faster reductive dissolution.

5.6. PURITY OF PLANT-DERIVED INDIGO (IV,V)

5.6.1. The optimization of extraction method (V)

The extraction method of plant-derived indigo from woad was optimised on a lab-scale. Different parameters of the process were studied to produce information on their effect on the indigo content and purity. The indigo content and purities were measured with spectrophotometric methods described in the experimental section.

The experiments showed that it is possible to increase the indigo content and purity by optimising the extraction method although the increase is highly dependent on the quality of leaf material. Two washings of the leaves were found out to increase the mean purity of indigo, however the purity stayed still under 50% which was very low when compared to the synthetic indigo. The impurities weren't examined in this experiment, and that could be interesting to see what constitutes the high impurity content and is there something in the method that might contribute to the impurities other than the high amount of calcium hydroxide present in the extractions. Even though the other bases might be more suitable to the method to lower the impurity content, calcium hydroxide was deemed necessary to use in the extractions because of its positive effect in the sedimentation of the indigo particles. According to Garcia-Macias and John [20] the calcium hydroxide act as nuclei in the formation of larger indigo particles which then sediment more quickly. The extraction time of 8 min was confirmed to be suitable to the hot extraction, as well as the fact that there is no need to adjust the pH of the steeping water to increase the indigo content or the purity.

The two temperatures of the extractions were studied and interestingly the cold extraction seems to give higher indigo contents than the hot extraction, although the purity is lower in the cold extraction. The higher content in cold extractions could be

due to the enzyme activity which is prevented in the hot extractions. However, more studies are needed to confirm that the cold extractions really give the higher indigo content or whether the result is due to the impurities disturbing the measurements. It would have quite an impact on the energy consumption of the extraction if it isn't necessary to heat the steeping water, this would also remove the need for cooling the water after the extraction. The fast cooling overall is not as necessary as it was thought to be initially, however the case might change with the larger scale of the extractions. The aeration time can be lowered to 15 min or even 5 min from the previously used 60 min, which is suitable to lowering the energy consumption. The aeration pH needs to be alkaline, the pH 11 seems to be the most suitable for the indigo production when both the indigo content and the purity are considered.

The indigo purity was mainly determined with the spectrophotometric method with NMP as a chosen solvent. The state of aggregation of the indigo in the solvent [6] may affect the method, and it has been suggested [55] that impurities in natural indigo reduce the size of indigo aggregates in solvents. Thus when pure synthetic indigo (larger aggregates) is used as a standard, the determinations of the impure natural indigo samples (finer aggregates) will overestimate the real indigo content. The voltammetric method was examined as a possible alternative for the conventional spectrophotometric method.

5.6.2. Sonovoltammetric determination of indigo purity (IV)

The *leuco*-indigo and indigo determination method based on voltammetry at a vibrating electrode described earlier was used for samples of impure plant-derived indigo from the optimisation of indigo extraction experiment. A comparison shows that the voltammetric method produces reliable results even when considerable amounts of ill-defined impurities are present. The results were compared to those obtained by the more conventional spectrometry. Initially, a calibration plot (limiting current versus indigo content) was obtained based on pure synthetic indigo samples at different temperatures (55, 65 and 75 °C). Reproducible data were obtained and the 75 °C conditions were selected for the determination of indigo in plant-derived indigo

samples. Figure 20 shows typical SEM images for the plant-derived indigo samples. At high magnification well-defined nanocrystalline indigo platelets are seen (see Figure 20 (B)) in between areas with inorganic impurities. It has been shown previously [20] by SEM-EDAX that impurities in plant-derived indigo are non-uniformly dispersed, and that soil and plant-derived particulates are responsible for persistent impurities in the final product.

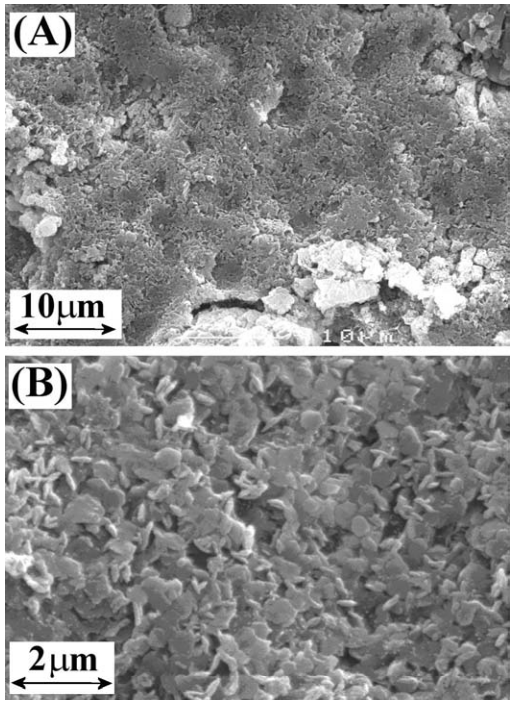

Figure 20. SEM data for plant derived indigo showing (A, B) secondary electron images for a typical sample at two different magnifications.

The leaf material from which the indigo is extracted is not homogeneous and there are many parameters which affect the indigo yield as well as the dye quality. For example, the growth conditions preceding harvest can significantly alter the indigo yield [141] and thus the impurity level [20]. The voltammetric analyses consistently indicate a purity less than that indicated by the spectrophotometric method (see Figure 21). Due to the known problems with the indigo aggregation in the solvents it was concluded that the voltammetric determinations of the indigo content of the natural indigo samples are the more accurate ones, and that the purity of the samples was typically 20-30%.

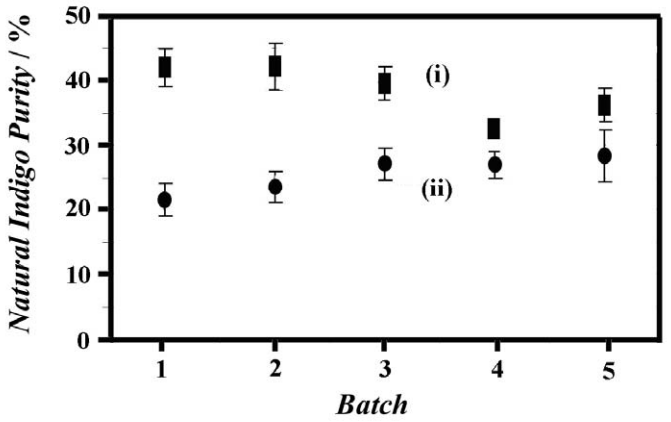

Figure 21. Histogram of the mean purity determined by spectrophotometry (i, rectangles) and determined by voltammetry (ii, circles) for each batch of plant material.

In support of the conclusion that the impurities are responsible for an overestimation by the spectrophotometric method, it was observed that when the impurity content is higher, the discrepancy between the two methods is greater, and the purer the samples, the closer are the values obtained with the two methods. The present results suggest that the voltammetric method is experimentally reproducible and more reliable than the spetcrophotometric method due to the complete dissolution of *leuco*-indigo and the reliable steady state voltammetric response at the vibrating electrode. Further work will be needed to determine the effect of indigoid impurities.

6. SUMMARY AND CONCLUSIONS

The reduction of indigo was studied with a mediator based system where DHAQ was used as a redox mediator. Another reduction method studied was glucose assisted reduction of indigo with and without catalyst. These reductions were both followed electrochemically. The effectiveness of the redox mediator DHAQ for the reduction of dispersed indigo has been investigated by rotating disc voltammetry. A detailed kinetic analysis produced with Digisim suggests that essentially, diffusion-controlled reduction occurs, and that at a temperature of 80 °C, DHAQ is an excellent mediator system for the reduction of dispersed indigo.

It was shown that hydrodynamic voltammetry (rotating disc and sonovoltammetry) offers a convenient and reliable tool for the determination of *leuco*-indigo in an alkaline bath containing indigo and glucose precursors. The methodology allowed a rate law and rate constant to be determined. It was demonstrated that anthraquinone, although insoluble in water, is a highly effective catalyst in the glucose-driven reduction of indigo to *leuco*-indigo in aqueous 0.1 M NaOH.

Anthraquinone was adsorbed/immobilised onto the indigo powder prior to the reduction. It was shown for indigo crystals of micron dimension, that a molar ratio of 1:400 for anthraquinone:indigo is effective for complete conversion with 10-fold excess of glucose at 65 °C. The temperature has a considerable effect on the anthraquinone-catalysed reductive dissolution. A molecular mechanism based on adsorption of anthraquinone between indigo sheets was proposed to explain the enhanced reductive dissolution. Anthraquinone and Na^+ ions are believed to penetrate between the indigo sheets and thereby help breaking up the solid crystal.

The sustainability of glucose as a reductant in indigo dyeing may be considered to be limited by the present high temperature requirement and a high alkalinity. However, the demonstration of a catalytic role for the anthraquinone points the way towards improvements that could be brought about in the glucose-driven process by the

identification of related compounds that combine an appropriate redox functionality and an ability to interact with the indigo particle surface.

The extraction method of plant-derived indigo from woad has been studied on a lab-scale. The results were compared to produce the method that would reduce the energy input as well as improve the product quality. More knowledge was produced on the effect of extraction process on the indigo content and purity even though the purity stayed under 50% which is still lower than the synthetic indigo.

A novel voltammetric determination method for indigo and/or *leuco*-indigo was developed employing a vibrating (250 Hz) 500 μm diameter gold disc electrode. Hydrodynamic voltammetry at a temperature of 75 °C was used to provide a well defined steady state current response for the quantitative determination of impure indigo samples. The reductive dissolution of indigo driven by glucose under alkaline conditions and at an elevated temperature of 75 °C allows *leuco*-indigo oxidation to be exploited and the limiting current to be used as a reliable measure of indigo content.

The sonoelectrochemical method developed was used for determination of indigo content in impure plant-derived indigo, but it is possible to utilize it also with other similar redox active substances. The two novel reduction methods developed in this study may be employed in the dyeing with indigo and possibly they could be applied to also other vat dyes. Synthetic indigo was mainly used in the redox experiments due to its homogeneity and purity. However, the results of this study may be used as a basis for further investigation of the reduction of plant-derived indigo and a possible development of more sustainable dyeing method of synthetic as well as plant-derived indigo.

7. ACKNOWLEDGEMENTS

The thesis work was carried out at the Plant Production Research of MTT Agrifood Research, at the Department of Chemistry in the University of Bath and the School of Biological Sciences in the University of Reading during the years 2004-2008. I am grateful for the funding from Finnish Cultural Foundation, Academy of Finland, SPINDIGO and MTT Agrifood Research Finland.

I would like to thank my supervisors, Dr Marjo Keskitalo at MTT and Dr Frank Marken at the University of Bath for invaluable support during the research. I would also like to thank Professor Keijo Haapakka for the opportunity to continue my studies at the University of Turku. I am also grateful for Professor Philip John for the possibility to do part of the research in Reading. I wish to express my gratitude also to all the co-authors for their contributions to the publications included in the thesis. I warmly acknowledge Professor Thomas Bechtold and Professor Fritz Scholz for their critical review of my thesis.

There are so many people that I would like to thank, who have been involved with my research either directly or in a more social role. My friends and colleagues in Finland and in England, you are in my thoughts. Special thanks go to Dr Susanna Muurinen for the inspiring discussions and support.

Finally many thanks to my family, parents Liisa and Jussi Vuorema, for supporting me through the years and my sister, Minna Vuorema-Chollat and her family for keeping things real.

Jokioinen, December 2008

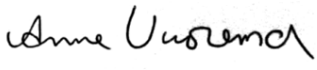

Anne Vuorema

8. REFERENCES

[1] Roessler, A.; Jin, X. State of the art technologies and new electrochemical methods for the reduction of vat dyes *Dyes and Pigm.* **2003**, *59*, 223-235.

[2] Roessler, A.; Crettenand, D. Direct electrochemical reduction of vat dyes in a fixed bed of graphite granules *Dyes and Pigm.* **2004**, *63*, 29-37.

[3] Clark, R.J.H.; Cooksey, C.J.; Daniels, M.A.M.; Withnall, R. Indigo, woad, and Tyrian Purple: important vat dyes from antiquity to present *Endeavour* **1993**, *17*, 191-199.

[4] Gilbert, K.G.; Cooke. D.T. Dyes from plants: Past usage, present understanding and potential *Plant Growth Regul.* **2001***, 34*, 57-69.

[5] Roessler, A.; Dossenbach, O.; Mayer, U.; Marte, W.; Rys, P. Direct Electrochemical Reduction of Indigo *Chimia.* **2001**, *55*, 879-882.

[6] Sandberg, G. *Indigo Textiles Technique and History,* Lark Books: Ashville **1989.**

[7] Padden, A.N.; John, P.; Collins, M.D.; Hutson, R.; Hall, A.R. Indigo-reducing *Clostridium isatidis* Isolated from a Variety of Sources, including a 10th-Century Viking Dye Vat *J. Archaeol. Sci.* **2000**, *27*, 953-956.

[8] Abdulla, S. Woad wage *Nature News* **1998**, Nov 26.

[9] Roessler, A.; Crettenand, D.; Dossenbach, O.; Rys, P. Electrochemical reduction of indigo in fixed and fluidized beds of graphite granules *J. Appl. Electrochem.* **2003**, *33*, 901-908.

[10] Bechtold, T.; Turcanu, A. Electrochemical Vat Dyeing Combination of an Electrolyzer with a Dyeing Apparatus *J. Electrochem. Soc.* **2002**, *149*, D7-D14.

[11] Bechtold, T.; Burtscher, E.; Kühnel, G.; Bobleter, O. Electrochemical reduction processes in indigo dyeing *J. Soc. Dyers Colour.* **1997**, *113*, 135-144.

[12] Roessler, A.; Crettenand, D.; Dossenbach, O.; Marte, W.; Rys, P. Direct electrochemical reduction of indigo *Electrochim. Acta* **2002**, *47*, 1989-1995.

[13] Blackburn, R.S.; Harvey, A. Green Chemistry Methods in Sulfur Dyeing: Application of Various Reducing D-Sugars and Analysis of the Importance of Optimum Redox Potential *Environ. Sci. Technol.* **2004**, *38*, 4034-4039.

[14] Ushida, S.; Matsuo, M. Reduction of indigo by glucose. *Nippon Kasei Gakkaishi.* **1991**, *42*, 61-65.

[15] Nicholson, S.K.; John, P. Bacterial indigo reduction *Biocatal. Biotransform.* **2004**, *22*, 397- 400.

[16] Nicholson, S.K.; John, P. The mechanism of bacterial indigo reduction *Appl. Microbiol. Biotechnol.* **2005**, *68*, 117-123.

[17] Hurry J.B. *The Woad Plant and its Dye*, Oxford University Press: London, **1930**

[18] Bechtold, T.; Burtscher, E.; Turcanu, A. Anthraquinones as mediators for the indirect cathodic reduction of dispersed organic dyestuffs *J. Electroanal. Chem.* **1999**, *465*, 80-87.

[19] Balfour-Paul, J. *Indigo,* British Museum Press: London, 2000.

[20] Garcia-Macias, P.; John, P. Formation of Natural Indigo Derived from Woad (*Isatis tinctoria* L.) in Relation to Product Purity *J. Agric. Food Chem.* **2004**, *52*, 7891-7896.

[21] Angelini, L.G.; Tozzi, S.; Nassi o Di Nasso, N. Effect of different sowing dates on leaf yield and indigo production of woad (*Isatis tinctoria* L.) in the mediterranean

environment. In: Pascual-Villalobos, M.J., Nakayama, F.S., Bailey, C.A., Correal, E., Schloman Jr., W.W. (Ed.) *Industrial Crops and Rural Development, Proceedings of the Annual Meeting of The Association for the Advancement of Industrial Crops*, 17-21 September 2005, Murcia, Spain, 535-545.

[22] Vandenabeele, P.; Moens, L.; Micro-Raman spectroscopy of natural and synthetic indigo samples *The Analyst* **2003**, *128*, 187-193.

[23] Seefelder, M. *Indigo in culture, science and technology*, Ecomed AG & Co. KG: Landsberg, **1994**.

[24] Christie, R.M. *Colour Chemistry,* The Royal Society of Chemistry: Cambridge, **2001**.

[25] O'Connor, K.E.; Hartmans, S. Indigo formation by aromatic hydrocarbon-degrading bacteria *Biotechnol. Lett.* **1998,** *20*, 219-223.

[26] Bhushan, B.; Samanta, S.K.; Jain, R.K. Indigo production by naphtalene-degrading bacteria *Lett. Appl. Microbiol.* **2000,** *31*, 5-9.

[27] Berry, A.; Dodge, T.C.; Pepsin, M.; Weyler, W. Application of metabolic engineering to improve both the production and use of biotech indigo *J. Ind. Microbiol. Biot.* **2002,** *28*, 127-133.

[28] Summary. Biotech bugs turn indigo blue in a green way. Application of metabolic engineering to improve both the production and use of biotech indigo *News@Nature* (25 Mar 2002), doi: 10.1038/news020325-4.

[29] Kokubun, T.; Edmonds, J.; John, P. Indoxyl derivatives in relation to medieval indigo production *Phytochemistry* **1998,** *49*, 79-87.

[30] Perkin, A.G.; Everest, A.E. *Natural Organic Colouring Matters.* Longmans, Green and Co.: London, 1918.

[31] Perkin, A.G.; Bloxam, W.P. CLXII. Indican. Part I *Transactions. J. Chem. Soc.* **1907,** *91*, 1715-1728.

[32] Oberthür, C.; Schneider, B.; Graf, H.; Hamburger, M. The Elusive Indigo Precursors in Woad (*Isatis tinctoria* L.) – Identification of the Major Indigo Precursor, Isatan A, and a Structure Revision of Isatan B *Chem. Biodiv.* **2004,** *1*, 174-182.

[33] Oberthür, C.; Graf, H.; Hamburger, M. The content of indigo precursors in *Isatis tinctoria* leaves- a comparative study of selected accessions and post-harvest treatments *Phytochemistry.* **2004,** *65*, 3261-3268.

[34] Maugard, T.; Enaud, E.; Choisy, P.; Legoy, M.D. Identification of an indigo precursor from leaves of *Isatis tinctoria* (Woad) *Phytochemistry.* **2001,** *58*, 897-904.

[35] Epstein, E.; Nabors, M.W.; Stowe, B.B. Origin of Indigo of Woad *Nature* **1967,** *216*, 547-549.

[36] Gilbert, K.G.; Hill, D.J.; Crespo, C.; Mas, A.; Lewis, M.; Rudolph, B.; Cooke, D.T. Qualitative Analysis of Indigo Precursors from Woad by HPLC and HPLC-MS *Phytochem. Analysis* **2000,** *11*, 18-20.

[37] Russell, G.A.; Kaupp, G. Oxidation of Carbanions. IV. Oxidation of Indoxyl to Indigo in Basic Solution *J. Am. Chem. Soc.* **1969,** *91*, 3851-3859.

[38] Stoker, KG.; Cooke, D.T.; Hill, D.J. An Improved Method for the Large-Scale Processing of Woad (*Isatis tinctoria*) for Possible Commercial Production of Woad Indigo *J. Agric. Engng Res.* **1998,** *71*, 315-320.

[39] Stoker, K.G.; Cooke, D.T.; Hill, D.J. Influence of light on natural indigo production from woad (*Isatis tinctoria*) *Plant Growth Regul.* **1998,** *25*, 181-185.

[40] Minami, Y.; Kanafuji, T.; Miura, K. Purification and characterization of a β-glucosidase from *Polygonum tinctorium*, which catalyzes preferentially the hydrolysis of indican *Biosci. Biotech. Bioch.* **1996,** *60*, 147-149.

[41] Hill, D.J. Preparation of indigo from woad *Beitrage zur Waidtagung.* **1992,** *4/5*, 23-26.

[42] Orchardson, I.Q.; Wood, S.H.; Bloxam, W.P. Analysis of indigo.-Part II *J. Soc. Chem. Ind.* **1907,** *26*, 4-10.

[43] Perkin, A.G.; Bloxam, W.P. XXX. Some constituents of natural indigo. Part I *Transactions. J. Chem. Soc.* **1907,** *91*, 279-288.

[44] Bechtold, T.; Turcanu, A.; Geissler, S.; Ganglberger, E. Process balance and product quality in the production of natural indigo from Polygonum tinctorium Ait. applying low-technology methods *Bioresource Technol.* **2002,** *81*, 171-177.

[45] Božič, M.; Kokol, V. Ecological alternatives to the reduction and oxidation processes in dyeing with vat and sulphur dyes *Dyes Pigm.* **2008,** *76*, 299-309.

[46] Roessler, A. *New electrochemical methods for the reduction of vat dyes,* Diss ETH No 15120. Zurich, **2003**.

[47] Domenech, A.; Domenech-Carbo, M.T.; Vazquez de Agredos Pascual, M.L. Indigo/ dehydroindigo/Palygorskite complex in Maya Blue *J. Phys. Chem. C.* **2007,** *111*, 4585-4595.

[48] Süsse, P.; Steins, M.; Kupcik, V. Indigo: Crystal Structure Refinement based on synchrotron data *Zeitschrift für Kristallographie* **1988,** *184*, 269-273.

[49] Steingruber, E. Indigo and Indigo colorants *Ullmann's Encyclopedia of Industrial Chemistry.* Online edition, Wiley-VCH Verlag GmbH & Co. KGaA. 2004.

[50] Green, L.R. The solubility of indigo *Dyes Hist. Archaeol.* **1989,** *8*, 15-16.

[51] Holt, S.J.; Sadler, P.W. Studies in enzyme cytochemistry III. Relationships between solubility, molecular association and structure in indigoid dyes *Proc. Royal Soc. London Ser. B Biol. Sci.* **1958,** *149*, 495-505.

[52] Monahan, A.R.; Kuder, J.E. Spectroscopic differences between crystalline and amorphous phases of indigo *J. Org. Chem.* **1972,** *37*, 4182-4184.

[53] Christie, R.M. Why is indigo blue? *Biotech. Histochem.* **2007,** *82*, 51-56.

[54] Aspland, J.R. A series on Dyeing, Chapter 3: Vat dyes and their application *Text. Chem. Color.* **1992,** *24*, 22-24.

[55] Novotna, P.; Boon, J.J.; van der Horst, J.; Pacakova, V. Photodegradation of indigo in dichloromethane solution *Color Technol.* **2003**, *119*, 121-127.

[56] Etters, J.N. Southeastern Section, AATCC. Effect of Dyebath pH on Color Yield in Indigo Dyeing of Cotton Denim Yarn *Text. Chem. Color.* 1989, *21*, 25-31.

[57] Johnson, A. (ed.) *The theory of coloration of textiles* Second edition, Society of Dyers and Colourists: Bradford, **1989**.

[58] Vickerstaff, T. *The physical chemistry of dyeing* Oliver and Boyd: London, **1954**.

[59] Etters, J..N. Indigo dyeing of cotton denim yarn: correlating theory with practice *J. Soc. Dyers Colour.* **1993**, *109*, 251-255.

[60] Etters, J.N. Advances in indigo dyeing: Implications for the dyer, apparel manufacturer and environment *Textile Chem. Colour.* **1995,** *27*, 17-22.

[61] Etters, J.N. Hou, M. Equilibrium sorbtion isotherms of indigo on cotton denim yarn: effect of pH *Textile Res. J.* **1991**, *61*, 773-776.

[62] Etters, J.N. pH-controlled indigo dyeing: buffered dyebaths vs caustic dosing *Am. Dyest. Rep.* **1998**, *87*, 15-17.

[63] Schlüter, H. Die vorteile der indanthren farbstoffe als kriterium für ihre segmentpezifische anwendung. *Textilveredlung.* **1990**, *25*, 218-221.

[64] Kulandainathan, M.A.; Patil, K.; Muthukumaran, A.; Chavan, R.B. Review of the process development aspects of electrochemical dyeing: its impact and commercial applications *Color. Technol.* **2007**, *123*, 143-151.

[65] Baumgarte, I. Vat dyes and their application *Rev. Prog. Color.* **1974**, *5*, 17-32.

[66] Bechtold, T.; Burtscher, E.; Amann, A.; Bobleter, O. Reduction of dispersed indigo dye by indirect electrolysis *Angew. Chem. Int. Ed. Engl.* **1992**, *31*, 1068-1069.

[67] Camacho, F.; Páez, M.P.; Jiménez, M.C.; Fernández, M. Application of the sodium dithionite oxidation to measure oxygen transfer parameters *Chem. Eng. Sci.* **1997**, *52*, 1387-1391.

[68] Etters, J.N. Efficient use of sodium hydrosulfite in commercial vat dyeing processes *Am. Dyest. Rep.* **1989**, *78*, 18-26.

[69] Semet, B.; Säckingen, B.; Grüningen, G.E. Eisen (II)-Salz-Komplexe als Alternative zu Hydrosulfit in der Küoen färberei *Melliand Textilber.* **1995**,*76*, 161-164.

[70] Chavan, R.B. Environment-friendly dyeing processes for cotton *Indian J. Fibre Text.* **2001**, *26*, 93-100.

[71] Meksi, N.; Kechida, M.; Mhenni, F. Cotton dyeing by indigo with the borohydride process: Effect of some experimental conditions on indigo reduction and dyeing quality *Chem. Eng. J.* **2007**, *131*, 187-193.

[72] Schnitzer, G.; Suetsch, F.; Schmitt, M.; Kromm, E.; Schlueter, H.; Krueger, R.; Weiper-Idelmann, A. Method of dyeing cellulose-containing textile material with hydrogenated indigo. *Europ. Pat.* EP 0 692 042 B1, **1996**.

[73] Padden, A.N.; Dillon, V.M.; John, P.; Edomnds, J.; Collins, M.D.; Alvarez, N. *Clostridium* used in mediaeval dyeing *Nature.* **1998**, *396*, 225.

[74] Padden, A.N.; Dillon, V.M.; Edmonds, J.; Collins, M.D.; Alvarez, N.; John, P. An indigo-reducing moderate thermophile from a woad vat, *Clostridium isatidis* sp. nov. *Int. J. Syst. Bacteriol.* **1999**, *49*, 1025-1031.

[75] Compton, R.G.; Perkin, S.J.; Gamblin, D.P.; Davis, J.; Marken, F.; Padden, A.N.; John, P. *Clostridium isatidis* colonised carbon electrodes: voltammetric evidence for direct solid state redox processes *New J. Chem.* **2000**, *24*,179-181.

[76] John, P. Indigo reduction in the woad vat: a medieval biotechnology revealed *Biologist.* **2006**, *53*, 31-35.

[77] Bond, A.M.; Marken, F.; Hill, E.; Compton, R.G.; Hügel, H. The Electrochemical reduction of indigo dissolved in organic solvents and as a solid mechanically attached to a basal plane pyrolytic graphite electrode immersed in aqueous electrolyte solution *J. Chem. Soc. Perkin Trans. II.* **1997**, *9*, 1735-1742.

[78] Komorsky-Lovrić, Š. Square-wave voltammetry of an aqueous solution of indigo *J. Electroanal. Chem.* **2000**, *482*, 222-225.

[79] Teli, M.D.; Paul, R.; Landage, S.M.; Aich, A. Ecofriendly processing of sulphur and vat dyes –An overview *Indian J. Fibre Text.* **2001**, *26*, 101-107.

[80] Bechtold, T.; Burtscher, E.; Turcanu, A.; Bobleter, O. Dyeing behavior of indigo reduced by indirect electrolysis *Textile Res. J.* **1997**, *67*, 635-642.

[81] Bechtold, T.; Burtscher, E.; Turcanu, A.; Bobleter, O. Indirect electrochemical reduction of dispersed indigo dyestuff *J. Electrochem. Soc.* **1996**, *143*, 2411-2416.

[82] Kulandainathan, M.A.; Muthukumaran, A.; Patil, K.; Chavan, R.B. Potentiostatic studies on indirect electrochemical reduction of vat dyes *Dyes Pigm.* **2007**, *73*, 47-54.

[83] Bechtold, T.; Burtscher, E.; Amann, A.; Bobleter, O. Alkali-stable Iron complexes as mediators for the electrochemical reduction of dispersed organic dyestuffs *J. Chem. Soc. Faraday Trans.* **1993**, *89*, 2451-2456.

[84] Bechtold, T.; Turcanu, A. Fe^{3+} -D-gluconate and Ca^{2+}-Fe^{3+} -D-gluconate complexes as mediators for indirect cathodic reduction of vat dyes –Cyclic voltammetry and batch electrolysis experiments *J. Appl. Electrochem.* **2004**, *34*, 1221-1227.

[85] Bechtold, T.; Burtscher, E.; Gmeiner, D.; Bobleter, O. The redox-catalysed reduction of dispersed organic compounds, Investigations on the electrochemical reduction of insoluble organic compounds in aqueous systems *J. Electroanal. Chem.* **1991**, *306*, 169-183.

[86] Bechtold, T.; Burtscher, E.; Turcanu, A.; Bobleter, O. The reduction of vat dyes by indirect electrolysis *J. Soc. Dyers Colour.* **1994**, *110*, 14-19.

[87] Bechtold, T.; Burtscher, E.; Bobleter, O. Application of electrochemical processes and electroanalytical methods in textile chemistry *Curr. top. Electrochem.* **1998**, *6*, 97-110.

[88] Bechtold, T.; Burtscher, E.; Bobleter, O.; Blatt, W.; Schneider, L. Optimization of multi-cathode membrane electrolysers for the indirect electrochemical reduction of indigo *Chem. Eng. Technol.* **1998**, *21*, 877-880.

[89] Roessler, A.; Dossenbach, O.; Marte, W.; Rys, P. Direct electrochemical reduction of indigo: process optimization and scale-up in a flow cell *J. Appl. Electrochem.* **2002**, *32*, 647-651.

[90] Roessler, A.; Dossenbach, O.; Marte, W.; Rys, P. Electrocatalytic hydrogenation of vat dyes *Dyes Pigm.* **2002**, *54*, 141-146.

[91] Roessler, A.; Rys, P. Electrochemical methods in the application of vat dyes *COLORCHEM' 02, 9th International Conference on pigments and dyes,* 12 - 16 May **2002**, Harmony Club Hotel Spindleruv Mlyn, Czech Republic.

[92] Ferrier, M.J.; Collins, P.M. *Monosaccharide chemistry* Penguin books: Harmondsworth, **1972**.

[93] de Bruijn, J.M.; Kieboom, A.P.G.; van Bekkum, H. Alkaline degradation of monosaccharides. Part VII. A mechanistic picture *Starch/Stärke* **1987**, *39*, 23-28.

[94] de Bruijn, J.M.; Kieboom, A.P.G.; van Bekkum, H. Reactions of monosaccharides in aqueous alkaline solutions *Sugar Technol. Rev.* **1986**, *13*, 21-52.

[95] Ghanem, M.A.; Compton, R.G.; Coles, B.A.; Canals, A.; Vuorema, A.; John, P.; Marken, F. Microwave activation of the electro-oxidation of glucose in alkaline media *Phys. Chem. Chem. Phys.* **2005**, *7*, 3552-3559.

[96] Bamford, C.H.; Collins, J.R.; Kinetic studies on carbohydrates in alkaline conditions. I. The kinetics of the autoxidation of glucose *P. Roy. Soc. Lond. A Mat.* **1950**, *204*, 62-84.

[97] Bamford, C.H.; Bamford, D.; Collins, J.R. Kinetic studies in alkaline condition. II. The kinetics of the rearrangements of glucose and fructose in alkaline solution *P. Roy. Soc. Lond. A Mat.* **1950**, *204*, 85-98.

[98] Bamford, C.H.; Collins, J.R. Kinetic studies on carbohydrates in alkaline conditions. III. Interconversion of D-glucose, D-fructose, D-mannose in feebly alkaline solution *P. Roy. Soc. Lond. A Mat.* **1955**, *228*, 100-119.

[99] Woo, H.J.; Sanseverino, J.; Cox, C.; Robinson, K.; Sayler, G. The measurement of toluene dioxygenase activity in biofilm culture of *Pseudomonas putida* F1 *J. Microbiol. Meth.* **2000**, *40*, 181-191.

[100] Akçakoca Kumbasar, E.P.; Aydin, H.; Ondogan, Z.; Ozcelik, M.; Ondogan, E.N. Automatic indigo measurement system as part of a dosing system for indigo dyeing *Fibres Text. East. Eur.* **2006**, *14*, 86-90.

[101] Şahin, U.; Ülgen, A.; Kekeç, A.; Gökmen, A. Real-time monitoring of indigo concentrations in the dyebath with a laser diode spectrometer *Textile Res. J.* **2004**, *74*, 193-197.

[102] Govaert, F.; Temmerman, E.; Westbroek, P. Determination of anthraquinone in alkaline sodium dithionite solution by electrochemical analysis *Anal. Commun.* **1998**, *35*, 153-156.

[103] Govaert, F.; Temmerman, E.; Kiekens, P. Development of voltammetric sensors for the determination of sodium dithionite and indanthrene/indigo dyes in alkaline solutions *Anal. Chim. Acta.* **1999**, *385*, 307-314.

[104] Westbroek, P.; De Clerck, K.; Kiekens, P.; Gasana, E.; Temmerman, E. Improving quality and reproducibility of the indigo dye process by measuring and controlling indigo and sodium dithionite concentrations *Textile Res. J.* **2003**, *73*, 1079-1084.

[105] Gasana, E.; Westbroek, P.; Temmerman, E.; Thun, H.P. Electrochemical behaviour of sodium dithionite at a platinum electrode and determination of diffusion coefficient in alkaline solution *Anal. Commun.* **1999**, *36*, 387-389.

[106] Manisankar, P.; Selvanathan, G.; Viswanathan, S.; Gurumallesh Prabu, H. Electrochemical Determination of some organic pollutants using wall-jet electrode *Electroanal.* **2002**, *14*, 1722-1727.

[107] Ghanem, M.A. ; Compton, R.G. ; Coles, B.A. ; Psillakis, E. ; Kulandainathan, M.A. ; Marken, F. Microwave activation of electrochemical processes : High temperature phenol and triclosan electro-oxidation at carbon and diamond electrodes *Electrochim. Acta.* **2007**, *53*, 1092-1099.

[108] Holt, K.B.; Del Campo, J.; Foord, J.S.; Compton, R.G.; Marken, F. Sonoelectrochemistry at platinum and boron-doped diamond electrodes: achieving 'fast mass transport' for 'slow diffusers' *J. Electroanal. Chem.* **2001**, *513*, 94-99.

[109] Compton, R.G.; Eklund, J.C.; Marken, F.; Waller, D.N. Electrode processes at the surfaces of sonotrodes *Electrochim. Acta* **1996**, *41*, 315-320.

[110] Scholz, F.; Schröder, U.; Gulaboski, R. *Electrochemistry of Immobilised Particles and Droplets* Springer-Verlag: Berlin Heidelberg, 2005.

[111] Bond, A.M.; Marken, F.; Williams, C.T.; Beattie, D.A.; Keyes, T.E.; Forster, R.J.; Vos, J.G. Unusually fast electron and anion transport processes observed in the oxidation of "electrochemically open" microcrystalline $[\{M(bipy)_2\}\{M'(bipy)_2\}(\mu\text{-}L)](PF_6)_2$ complexes (M,M'=Ru, Os; bipy=2,2'-bipyridyl; L=1,4-dihydroxy-2,5-bis(pyrazol-1-yl)benzene dianion) at a solid-electrode-aqueous electrolyte interface *J. Phys. Chem. B.* **2000**, *104*, 1977-1983.

[112] Grygar, T.; Marken, F.; Schroder, U.; Scholz, F. Electrochemical analysis of solids. A review *Collect. Czech. Chem. Commun.* **2002**, *67*, 163-207.

[113] Rudolph, M.; Reddy, D.; Feldberg, S.W. A simulator for cyclic voltammetric responses *Anal. Chem.* **1994**, *66*, 589A-600A.

[114] Compton, R.G.; Brown, C.A. Monitoring particle sizes with rotating disc electrodes: measurement of the dissolution kinetics of calcite *J. Colloid Interface Sci.* **1993**, *158*, 243-246.

[115] Marken, F.; Compton, R.G. Sonoelectrochemically modified electrodes: ultrasound assisted electrode cleaning, conditioning, and product trapping in 1-octanol/water emulsion systems *Electrochim. Acta.* **1998**, *43*, 2157-2165.

[116] Angelini, L.G.; John, P.; Tozzi, S.; Vandenburg, H. Extraction of indigo from *Isatis tinctoria* L. and *Polygonum tinctorium* Ait. as a basis for large-scale production. In: Pascual-Villalobos, M.J., Nakayama, F.S., Bailey, C.A., Correal, E., Schloman Jr., W.W. (Ed.) *Industrial Crops and Rural Development, Proceedings of the Annual Meeting of The Association for the Advancement of Industrial Crops,* 17-21 September **2005**, Murcia, Spain, 521-534.

[117] Green, L.R.; Daniels, V.D. The use of N-methyl-2-pyrrolidone (NM2P) as a solvent for the analysis of indigoid dyes *Dyes Hist. Archaeol.* **1992**, *11*, 10-18.

[118] Fernández-Sánchez, C.; Costa-García, A. Voltammetric studies of indigo adsorbed on pre-treated carbon paste electrodes *Electrochem. Commun.* **2000**, *2*, 776-781.

[119] Brett, C.M.A.; Brett, A.M.O. *Electrochemistry principles, methods, and applications* Oxford University Press: Oxford 1993.

[120] Atkins P.W. *Physical Chemistry.* Oxford University Press: Oxford, 1998.

[121] Grygar, T.; Kučkova, Š.; Hradil, D.; Hradilová, D. Electrochemical analysis of natural solid organic dyes and pigments *J. Solid State Electrochem.* **2003**, *7*, 706-713.

[122] Oldham, K.B.; Myland, J.C. *Fundamentals of Electrochemical Science* Academic Press Inc.: San Diego, 1994.

[123] Walsh, F. *A first course in electrochemical engineering* The Electrochemical Consultancy: Romsey, 1993.

[124] Forryan, C.L.; Klymenko, O.V.; Brennan, C.M.; Compton, R.G. Reactions at the solid-liquid interface: Surface-controlled dissolution of solid particles. The dissolution of potassium bicarbonate in dimethylformamide *J Phys. Chem. B.* **2005**, *109*, 2862-2872.

[125] Forryan, C.L.; Klymenko, O.V.; Wilkins, S.J.; Brennan, C.M.; Compton, R.G. Experimental and theoretical study of the surface-controlled dissolution of cylindrical particles. Application to solubilization of potassium hydrogen carbonate in hot dimethylformamide *J Phys. Chem, B.* **2005**, *109*, 20786-20793.

[126] Süsse, P.; Wolf, A. A new crystalline phase of indigo *Naturwissenschaften* **1980**, *67*, 453.

[127] Grimme, G.; Grimme, S.; Jones, P.G.; Boldt, P. AM1 and X-ray studies of the structures and isomerization reactions of indigo dyes *Chem. Ber.* **1993**, *126*, 1015-1021.

[128] Akkermans, R.P.; Wu, M.; Compton, R.G. A comparison between pulsed sonovoltammetry and low power laser activated voltammetry for the electroanalysis of ascorbic acid in a commercial fruit drink *Electroanal.* **1998**, *10*, 814-820.

[129] Akkermans, R.P.; Roberts, S.L.; Marken, F.; Coles, B.A.; Wilkins, S.J.; Cooper, J.A.; Woodhouse, K.E.; Compton, R.G. Methylene green voltammetry in aqueous solution: Studies using thermal, microwave, laser, or ultrasound activation at platinum electrodes *J. Phys. Chem. B.* **1999**, *103*, 9987-9995.

[130] Marken, F.; Eklund, J.C.; Compton, R.G. Voltammetry in the presence of ultrasound: can ultrasound modify heterogeneous electron transfer kinetics? *J. Electroanal. Chem.* **1995**, *395*, 335-339.

[131] Chapman, C.S.; van den Berg, C.M.G. Anodic stripping voltammetry using a vibrating electrode *Electroanal.* **2007**, *19*, 1347-1355.

[132] Kubota, N.; Tanigawa, M.; Shimoda, K.; Fujii, S.; Tatsumoto, N.; Sano, T. Effect of potential scan rate on electro-redox reaction in ultrasonic vibrating electrode-voltammetry *Anal. lett.* **2003**, *36*, 2539-2550.

[133] Williams, D.E.; Ellis, K.; Colville, A.; Dennison, S.J.; Laguillo, G.; Larsen, J. Hydrodynamic modulation using vibrating electrodes: Application to electroanalysis *J. Electroanal. Chem.* **1997**, *432*, 159-169.

[134] Mikkelsen, Ø.; Schrøeder, K.H. An oscillating and renewing silver electrode for Cadmium and Lead detection in differential pulse stripping voltammetry *Electroanalysis* **2001**, *13*, 687-692.

[135] Scholz, F. *Electroanalytical Methods, Guide to Experiments and Applications* Springer-Verlag: Berlin Heidelberg, 2002.

[136] Sur, U.K.; Marken, F.; Rees, N.; Coles, B.A.; Compton, R.G.; Seager, R. Microwave enhanced electrochemistry: mass transport effects and steady state voltammetry in the sub-millisecond time domain *J. Electroanal. Chem.* **2004**, *573*, 175-182.

[137] Bard, A.J.; Inzelt, G.; Scholz, F. *Electrochemical Dictionary* Springer-Verlag: Berlin Heidelberg, 2008.

[138] Compton, R.G.; Banks, C.E. *Understanding Voltammetry* World Scientific Publishing Co. Pte. Ltd: Singapore, 2007.

[139] Wilke, C.R.; Chang, P. Correlations of diffusion coefficients in dilute solutions *A.I.Ch.E. Journal* **1955**, *1*, 264-270.

[140] Budavari, S. (ed.) *The Merck Index,* 12th ed., Merck & Co: New Jersey, 1996.

[141] Campeol, E.; Angelini, L.G.; Tozzi, S.; Bertolacci, M. Seasonal variation of indigo precursors in *Isatis tinctoria* L. and *Polygonum tinctorium* Ait. as affected by water deficit *Environ Exp Botany* **2006**, *58*, 223-233.